Monthly Notices of the Royal Astronomical Society

MNRAS **537,** 2763–2781 (2025) https://doi.org/10.1093/mnras/staf079
Advance Access publication 2025 January 21

Eruptive YSOs in Cygnus-X: a mid-infrared variability study with NEOWISE and SPICY

C. Morris,[1★] Z. Guo,[1,2,3] P. W. Lucas,[1] N. Miller,[4] C. Contreras Peña[5,6] and M. A. Kuhn[1]

[1]Centre for Astrophysics Research, University of Hertfordshire, College Lane, Hatfield, Hertfordshire AL10 9AB, UK
[2]Instituto de Física y Astronomía, Universidad de Valparaíso, ave. Gran Bretaña, 1111, Casilla 5030, Valparaíso 2362735, Chile
[3]Millennium Institute of Astrophysics, Nuncio Monseñor Sotero Sanz 100, Of. 104, Providencia, Santiago7820436, Chile
[4]Department of Physics and Astronomy, University of Wyoming, 1000 E. University, Laramie, WY 82070, USA
[5]Department of Physics and Astronomy, Seoul National University, 1 Gwanak-ro, Gwanak-gu, Seoul 08826, Republic of Korea
[6]Research Institute of Basic Sciences, Seoul National University, Seoul 08826, Republic of Korea

Accepted 2025 January 7. Received 2025 January 6; in original form 2024 August 29

ABSTRACT

The mass accretion process controls pre-main-sequence evolution, although its intrinsic instability has yet to be fully understood, especially towards the protostellar stage. In this work, we have undertaken a thorough examination of the mid-infrared (MIR) variability of *Spitzer*-selected young stellar objects (YSOs) in the Cygnus-X star-forming region over the last decade, using the Near-Earth Object Wide-field Infrared Survey Explorer time series. This work compares two groups of young stars: embedded Class I objects, and the more evolved flat-spectrum/Class II sources. We report on 48 candidate eruptive variables within these groups, including 14 with characteristics that resemble the photometric behaviour of FUors. We also include an additional 20 YSOs, which are of a less certain categorization. We find the candidate FUors to be an order of magnitude more common among the younger Class I systems than more evolved objects. A large number of the identified short-duration eruptive YSOs display MIR colour behaviour that is redder-when-brighter, which contrasts with optically bright outbursts seen in YSOs. Finally, we note the unusual long-term rising behaviours of four Class I YSOs, with rise time-scales longer than 5 yr, which is far slower than ∼6–12 month time-scale for the majority of optically discovered FUors. Additionally, our broader investigation of MIR variability for embedded Class I YSOs shows that there is a higher incidence of high-amplitude variability for these stars, than is seen in Class II sources. This holds true for all variable Class I YSOs, not just the eruptive sources.

Key words: stars: pre-main sequence – stars: protostar – stars: variables: T Tauri, Herbig Ae/Be – infrared: stars.

1 INTRODUCTION

Pre-main-sequence evolution of low-mass stars consists of four stages (from Class 0 to III), defined by the relative brightness of the stellar photosphere and the circumstellar disc or envelope (Greene & Lada 1996). Class 0 and Class I sources are the earliest evolutionary stages, so-called protostars, during which the young star is embedded in its envelope and optically invisible. During the more evolved Class II stage, the young stellar object (YSO) is directly observable at optical wavelengths, accompanied by active accretion funnel flows linking the circumstellar disc and the stellar surface (Bouvier et al. 2007). Additionally, the 'flat-spectrum' stage (FS) is defined as the transitional stage between Class I and II, where the stellar photosphere and accretion disc share similar luminosity, namely a flat spectral energy distribution (SED). Quantitatively, these pre-main-sequence evolutionary stages were classified by the near to mid-infrared (MIR) spectral index α, as Class I ($\alpha > 0.3$), FS ($-0.3 < \alpha < 0.3$), and Class II ($\alpha < -0.3$). Previous photometric surveys have revealed that the mass accretion process on YSOs has an inherent instability (e.g. Stauffer et al. 2014; Venuti et al. 2019; Contreras Peña et al. 2020). However, most past works focused on the optical to near-infrared (NIR) variability of Class II YSOs. Systematic monitoring of the accretion variability of protostellar cluster members will shed light on the accretion variability towards earlier evolutionary stages, where the average accretion rate is higher than in the FS and Class II stages (see the models used in Fischer et al. 2017).

The long duration time coverage of MIR surveys, by *Spitzer*, *WISE*, and the current Near-Earth Object Wide-field Infrared Survey Explorer (NEOWISE, Hora et al. 2007; Wright et al. 2010; Mainzer et al. 2014), provides the ability to find variable events on multiyear time-scales. The nearby massive star-forming complex of Cygnus-X (at roughly 1.4 kpc, Rygl et al. 2012) makes an excellent test site for studying the long-term behaviour of YSOs, because of the wide range of surveys it is included within. These surveys cover multiple wavelengths with a long time baseline, providing a high completeness of YSO candidates in the region. The large sample of Kryukova et al. (2014), which identifies over 2000 candidate YSOs, utilized the full MIR coverage provided by *Spitzer* to isolate YSO candidates on the basis of MIR colour; these sources are exclusively Class I YSOs with a 24 μm ([24]) detection. The same sky region is also covered by

★ E-mail: c.morris6@herts.ac.uk

NEOWISE, The UKIRT Galactic Plane Survey (UGPS) (Lucas et al. 2008), the Two Micron All-Sky Survey (2MASS) (Skrutskie et al. 2006), *Gaia* (Gaia Collaboration. 2023), and the INT Photometric Hα Survey (Drew et al. 2005; Barentsen et al. 2014).

In addition, there is a large list of YSO candidates available in the Cygnus-X region, from the *Spitzer*-based SPICY (Kuhn et al. 2021) catalogue of YSOs. SPICY uses a mixture of traditional infrared colour cuts and random forest classifiers to produce a comprehensive list of Class II and FS YSOs in the 613 deg^2 covered by the existing cryogenic-era Glimpse surveys (Benjamin et al. 2003; Whitney et al. 2011). It contains a large number of Class I YSOs and a reduced number of Class III sources owing to the much lower IR excess of those stars. In this instance, there are 7281 additional YSOs, to those found in the aforementioned sample from the Cygnus-X Legacy Survey (Beerer et al. 2010; Kryukova et al. 2014).[1] Given the broad wavelength coverage of the region, there lies an opportunity to investigate the range and frequency of both high-amplitude variability generally and eruptive variability specifically, for YSOs at different evolutionary stages.

The post-reactivation NEOWISE survey provides an opportunity to study the long-term time-domain behaviour of YSOs. The NEOWISE survey covers the whole sky in both the 3.4 µm $W1$ and 4.6 µm $W2$ bands. At present, there have been over 10 yr of continuous monitoring, at ∼6 month intervals, comprised of many single scans. Considering the higher brightness at 24 µm of the Class I protostars, our sample of Class I YSOs will preferentially target the younger objects. Such a search for eruptive variables (EVs) at the protostellar stage has not been previously carried out within Cygnus-X.

Variability is a common characteristic among YSOs. This is often of a low amplitude nature (<1 mag in optical), driven by small changes in extinction along line of sight, accretion rate, or by stellar rotation. Alternatively, unpredicted high-amplitude accretion events are observed on young stars, during which YSOs accrete a significant portion of their final mass (see Hartmann & Kenyon 1996). These bursts have a myriad of different triggering mechanisms, with theoretical studies able to reproduce outbursts via: gravitational Instability (GI) and magnetorotational instability (MRI) in the inner disc (Kratter & Lodato 2016; Bourdarot et al. 2023), thermal instabilities (Bell & Lin 1994; Nayakshin & Elbakyan 2024), disc fragmentation, either due to GI (Vorobyov & Basu 2010), or young massive planets (Clarke et al. 2005), stellar flybys (Cuello et al. 2019; Borchert et al. 2022b), and evaporating young hot Jupiter (Nayakshin et al. 2024). This wide range also ensures that there is no universal model for an episodic accretion event, and thus large observationally confirmed samples of these events will be required to understand them further.

Observationally, the young accretion bursts are traditionally characterized into two distinct groups, based on their duration and amplitude. The FUor-type, named after FU Ori, are long-lasting (order of decades or centuries) outbursts of high amplitude and a comparatively short brightening time-scale, of the order of ∼1000 d (Hartmann & Kenyon 1996). These outbursts are considered rare, with only a few dozen confirmed by both spectroscopy and photometry (Connelley & Reipurth 2018), including those recently identified by VVV and *Gaia* time series photometry (such as Contreras Peña et al. 2017a; Hillenbrand et al. 2018; Lucas et al. 2024; Guo et al. 2024a, b). More recent works (such as Contreras Peña et al. 2023; Park et al. 2024; Tran, De & Hillenbrand 2024) have made use of the NEOWISE time series to identify younger or more heavily embedded FUor candidates, with a view to increasing the number of systems known. The NEOWISE stacked image catalogue unTimely has also been used for this purpose (Li & Wang 2024). Additionally, the survey of Park et al. (2021a) quantified the array of variabilities seen in YSOs with NEOWISE (although the majority of those authors outbursting sources were Class II YSOs). The recurrence time-scales of FUors are of the order of 10^5 yr (Scholz, Froebrich & Wood 2013). These outbursts are driven by massively enhanced accretion (crushing the magnetic field of the star), which will then cause the inner accretion disc to become self-luminous via viscous heating, and outshine the young star's photosphere, hence the distinctive spectrum of these objects (Zhu et al. 2009; Hartmann, Zhu & Calvet 2011; Liu et al. 2022). Unlike FUors, there is another type of young outbursting stars called EXors. These have a much shorter outburst duration of between months and a few years as well as a symmetric rising/cooling light-curve morphology (Lorenzetti et al. 2012). Some EXors have repeated outbursting behaviour on a time-scale of a decade (Kuhn et al. 2023) and some others may be periodic (Guo et al. 2022). Uniform amongst EXors is that the YSOs maintain magnetospheric accretion (i.e the YSO's magnetic field is not crushed by the accreting material, and thus boundary layer accretion continues), with spectra frequently containing H I emission lines (Contreras Peña et al. 2017b; Guo et al. 2020). Recently, a much wider array of outbursting behaviours has been noted among eruptive YSOs (reviewed by Fischer et al. 2022), consisting of YSOs with photometric features similar to FUors, but with spectroscopic traits more comparable to EXors (see Briceño et al. 2004; Acosta-Pulido et al. 2007). The range of behaviours is further challenged by the NIR VVV survey (Minniti et al. 2010; Guo et al. 2021), where the majority of long-duration outbursts (>10 yr) were displaying EXor-like magnetospheric accretion signatures in their spectra. More recent literature has referred to intermediate duration outbursts as V1647 Ori-type (see table 1 in Fischer et al. 2022), which do not fit into the classical EXor or FUor groups. V1647 Ori-type (also referred to as MNors) outbursts are of interest in this work, owing to their similarities to both FUors and EXors. These similarities pertain to both their intermediate duration (faster than those of classical FUors but longer than EXors) and their mixed spectral features (often featuring emission lines). The durations are of further note because of the number of newly discovered FUors with <10 yr outbursts. See Briceño et al. (2004), Aspin et al. (2009), Ninan et al. (2013), and Park et al. (2021b, 2022) for further discussion on the group and of V1647 Ori in general.

The incidence rate of eruptive variability in YSOs is a subject of importance when considering the 'protostellar luminosity spread problem', but the variance in amplitude (with respect to the photometric bandpasses being used for observations) has not been probed in detail previously. Statistical studies using large-scale photometric surveys revealed that accretion outbursts are more common at younger stages, with a lower occurrence rate towards more evolved systems (see Contreras Peña et al. 2024). However, driven by the larger amplitudes observed in the optical and near-IR (as compared to those found in the MIR), YSOs with a less massive envelope are easier to detect during the outburst, leading to a bias on the estimated number density.

Most eruptive YSOs have amplitudes ≥2 mag in NIR surveys (see Guo et al. 2024a), although there is a significantly higher ceiling than this (e.g. $\Delta W2 = 8$ mag Lucas et al. 2020). We calculated amplitudes of a large number of confirmed EVs from the Outbursting YSOs CATalogue (OYCAT; Contreras Peña et al., in preparation). We find

[1]The data release document can be found here: https://lweb.cfa.harvard.edu/cygnusX/.

that EVs in the optical/NIR bandpasses have a median amplitude of 3.3, 4.0, 3.2 mag in the G, R, and K_s filters, respectively.

A sample of nearby YSOs, selected from the MIR NEOWISE photometry, is desired to examine the range of eruptive behaviours towards the younger evolutionary stage. We have performed a detailed survey to monitor the long-term time-domain behaviour of these young systems, providing insight into how common the traditional FUor and EXor variables might be among a MIR-selected population, or if other eruptive events will dominate.

In this work, we will present two selections of YSOs within the region of Cygnus-X. Sample (1) consists of embedded objects with a 24 μm detection, mostly Class I YSOs with a small number of FS stars. Sample (2) is comprised of non-embedded FS and Class II/III sources (likely without envelopes), taken from The *Spitzer*/IRAC Candidate YSO Catalogue (SPICY; Kuhn et al. 2021). The details of our sample selection methods and data-processing procedures are presented in Section 2. In Section 3, we will discuss individual EVs of interest within each selection. Then, in Section 4, we will compare the incidence of eruptive variability (and of the FUor phenomenon, in particular) between both populations and of similar sources from the literature.

2 SAMPLE SELECTION AND DATA PROCESSING

In this section, we will present the data products applied in this work, including archived data products from the *WISE* satellite and PI observations for highlighted sources. We will also introduce our selection methods to identify eruptive YSOs among the members of the Cygnus-X star-forming region.

2.1 Archived *WISE* data

We obtained NEOWISE light curves from the NASA/IPAC InfraRed Science Archive for the 2007 YSO candidates in Cygnus-X (Kryukova et al. 2014), among which 1552 sources have a detection in at least one epoch of the time series, in both *W1* and *W2*. Of these 1552 sources, 1332 (these forming our first sample) have detections in at least 50 per cent of the possible epochs of single scan data. We use the terms 'scan' and 'epoch' with regard to the NEOWISE time series to refer to the multiple single images (scans) that are taken over the course of a few weeks, this being repeated ∼2 times per year (epochs). For each of the 1332 light curves, the NEOWISE single-scan data were combined with the earlier *WISE* measurements (ALLWISE, *WISE* 3-Band Cryo, and Post-Cryo, where available, acquired from the ALLWISE Multi-Epoch Photometry Table). The photometry from the individual scans was then cleaned by removing detections with a high psf error. Additionally, those points with either *w1snr* or *w2snr* <5 were subject to cuts first used in Koenig & Leisawitz (2014):

$$w1rchi2 < \frac{w1snr - 3}{7}, \tag{1}$$

$$w2rchi2 < (0.1 \times w2snr) - 0.3. \tag{2}$$

Data points that did not pass either criterion were not included in the per epoch median magnitudes. The error bars were taken as the standard deviation for the cleaned single-scan images at each epoch, rather than the stated photometric error in the catalogue. This change was motivated by the larger spread in fluxes at each epoch than the stated errors, which may be indicative of an underlying underestimate of errors in the NEOWISE data. In this work, we measured the standard deviation of the aforementioned spread to be 0.22 mag for the $W1$ bandpass, and 0.15 mag in $W2$. These values are obtained by first finding the average scatter in each 'epoch' for a given star, then retrieving the standard deviation in this value across the whole sample. There is no clear magnitude dependence on the scattering within our sample. We also note that since most of our targets are faint sources located in crowded fields, they have systematically larger spreads per epoch compared with the brighter and more isolated *WISE* sources (see e.g. Lucas et al. 2024). Additional data cleaning involved removing photometric measurements associated with quality control flags attributed to the frame itself ($'\mathrm{qual\_frame}' \neq 0$) or those had measured fluxes as upper limits only.

To remove any bias associated with the selection of more heavily embedded YSOs (as well as investigating the distribution of EVs within this regime), a counterpart sample of sources was selected from the SPICY catalogue (Kuhn et al. 2021), featuring all candidate YSOs within the sky area used by Kryukova et al. (2014), that did not feature in those authors' sample. This SPICY sample includes 7281 stars that were not recognized by Kryukova et al. (2014), of which 5592 possess NEOWISE light curves, and 4935 have data of sufficient quality for analysis. We deem that a star must have data in at least 40 per cent of epochs to reliably analyse in this regard.

Both the binned (the median of each scan within a single observation window) and unbinned light curves in the first sample (1332) were visually inspected to locate eruptive YSOs. Eruptions were considered for stars with amplitudes of over 1 mag, in either *WISE* bandpass (corresponding to ∼2 mag in optical band-passes), and obvious brightening from a quiescent state, leaving 299 light curves. Some sample members were further examined via the inspection of their unTimely (Meisner et al. 2023) light curves, generated with the untimely catalogue tool (Kiwy 2022). The untimely catalogue is the time series of unWISE (Meisner, Lang & Schlegel 2018), which stack the individual NEOWISE sky-passes to create deeper (∼ 1.3 mag) per epoch images, using the `crowdsource` source detection and photometry software (Schlafly et al. 2018). The sources examined here were those with clearly variable light curves but with either high photometric error or a number of non-detections.

Candidate long-duration eruptive YSO outbursts were identified by fitting the light curves to a characteristic shape, defined by the rising slope, and a post-outburst linear decay. The two-component rising slope is defined in equations (3) and (4), as listed in Lucas et al. (2024):

$$m(t) = m_\mathrm{q} - \frac{s}{1 + \mathrm{e}^{-(t-t_0)/\tau}} \quad \text{where} \quad t < t_0, \tag{3}$$

$$m(t) = m_\mathrm{q} - s(0.5 + 0.25(t - t_0)/\tau) \quad \text{where} \quad t_0 \leq t \leq t_0 + 2\tau, \tag{4}$$

where $m(t)$ is magnitude as a function of time (t), m_q is the magnitude at quiescence, t_0 is the time at which the star is at half the peak amplitude (s), and τ is the e-folding time-scale. The fitting combines the above formalism with a linear decay that runs from $t_0 + 2\tau$ to the end of the time axis. The fit itself makes use of SCIPY's `curvefit` routine, using the above model, to fit the initial guesses for five free parameters (τ, t_0, m_q, s, and the final magnitude), that are then fit by EMCEE over 10 000 iterations (this code is now packaged as part of `aptare`[2]). The sources with the lowest reduced mean squared error are then inspected to confirm as the FUor-type (examples are

[2]Available at https://github.com/nialljmiller/Aptare.

presented in Appendix A). We employed a cut-off value in root mean-squared error (RMSE > 0.1) between the fit and the normalized light curve to separate the candidates. This value is calculated from flux normalized between 0 and 1, and not the original apparent magnitude, and the RMSE is a measure of the average deviation (in this instance not more than 10 per cent of the amplitude). We note that this cut did lead to 2 likely genuine eruptive targets (considered as such from their amplitudes and overall morphology) failing the cut, which were re-confirmed by visual inspections. This method does struggle to identify sources with bursts at the start of the NEOWISE monitoring window, as well as those that are currently rising (or very recently finished), such as Source 2003. It should be noted that all stars that were identified as EV candidates by visual inspection were still subject to analysis and that this fitting method was trialled to locate YSOs resembling classical FUors.

We also utilized the two-epoch UGPS survey (Lucas et al. 2008; Lucas et al. 2017) to identify YSOs with earlier outburst events (these being between 2011 and 2012) than would be seen between the epochs of the *Spitzer* Cygnus-X Legacy Survey and ALL-WISE/NEOWISE surveys. We selected members of the Kryukova et al. (2014) catalogue featuring a detection in 50 per cent of UGPS images, then visually inspected the images to confirm genuine variability. This search identified 15 candidates, of which 11 were of sufficiently high amplitude ($>$ 2 mag in K) to be considered eruptive. Of those 11, only two were not picked up by the NEOWISE search method (see Section 3).

The techniques detailed in this section were focused on identifying FUor-type behaviour primarily, because of their rarity and the long time-scale of these outbursts. EXor-type YSOs were still important in this work and will be discussed further below. The fitting methods above do not suit the shorter outbursts of these stars and would be challenging to distinguish from quasi-periodic and aperiodic dippers in many (but not all) cases.

2.2 Additional data products

We present three K-bandpass spectra of two candidate EVs identified via the large flux differences between two photometric epochs of the UKIDSS survey (Lucas et al. 2017). Two spectra were obtained by the Near-Infrared Integral Field Spectrometer (NIFS) mounted on the Gemini North telescope (McGregor et al. 2003), in 2013 June and December. Another spectrum was observed in 2017 July with the Infrared Camera and Spectrograph (IRCS) installed at the *Subaru* telescope (Tokunaga et al. 1998; Kobayashi et al. 2000). The IRCS spectrum was reduced using the standard `twodspec` routines within IRAF, and it has a resolution of 6.1 Å per pixel. The NIFS spectra were originally reduced by and part of the published PhD thesis of Carlos Contreras Peña (Contreras Peña 2015).

3 RESULTS

We present 68 candidate EVs, across both the groups, those with MIPS [24] detections and those SPICY selected stars without them. They are to be split into three classifications based on their outburst time-scales (which are predicted in instances where the latest event is ongoing). The three groups are 'Long-Duration' of $>$10 yr (LDE), 'Intermediate-Duration' of $2 \leq t \leq 10$ yr (IDE), and 'Short-Duration' which are $<$2 yr (SDE). Overall, we identified 13 'Long-Duration' YSO outbursts, with 9 of 'Intermediate-Duration' and 41 'Short-Duration' events (these events were solely identified by eye). A final five of the YSOs with ongoing outbursts at the final epoch had not been active long enough to classify in this way, and are listed as 'ambiguous'. These time-scale-based classifications are based on those used in Contreras Peña et al. (2024), although the cuts for short and intermediate durations have been slightly modified (less and greater than 1 yr has now been changed to 2 yr). This change was carried out to reflect the slightly variable sampling rate of NEOWISE making it somewhat challenging to reliably determine if an outburst is less than a year or a year and a half.

3.1 Stars with MIPS [24] detection

There are 33 EVs that have MIPS [24] detection (which can be viewed in Table 2), and have an ID derived from the Vizier row number for the Kryukova et al. (2014) catalogue. Most of the stars are Class I YSOs (28) and a small number of FS sources (5). The FS sources in this sample require $[3.6] - [4.5] \geq 0$, as per Kryukova et al. (2014). These sources were sorted into the three aforementioned categories based on the outburst time-scale, as 11 long-duration, 8 intermediate-duration, and 11 short-duration outbursts. There are a final three star that are of an ambiguous categorization: sources 2003, 1738, and 1769. The former has a notably high amplitude ($>$ 5 mag in $W1$), but as per the latest NEOWISE release the outburst is still ongoing, and thus of an unknown type and duration. By contrast, Sources 1738 and 1769 have had multiple events observed in their light curves. For both systems, one burst appears as a long/intermediate duration type (ongoing as of 2024), and the other was a short-duration burst. Two additional stars (Sources 362 and 1964) are included in this group which were detected as candidate eruptive stars via the two-epoch UGPS survey (Lucas et al. 2017). All eruptive targets can be found in Table 1. The time-scales in question are estimates, with two methods used: for SDEs and IDEs these are taken from the time between the start of the event and the point of return to the quiescent magnitude. For the LDEs, the time-scale is the fitted τ from equation (3), unless the star has a plateau-like post-rise feature, in which case the time-scale is stipulated to be greater than 10 yr long.

3.1.1 Long-duration eruptive YSOs

Within the group of 11 EVs with variability time-scales greater than 10 yr, we note the presence of four stars with morphologies with similarities to those of classical FUors (numbers: 257, 294, 591, and 1475, see Figs 1 and B1), i.e with a high-amplitude outburst, that increases in brightness comparatively fast when compared to the following long duration decay. All display a high amplitude increase in luminosity over a 1–5 yr period, followed by a plateauing that appears set to continue long into the future. Sources 257 and 294 show no signs of post-outburst fading, whereas source 1475 has an estimated fading time-scale of $\approx$ 24 yr assuming a linear decaying slope. Source 257 appears of a V1647 Ori-type on the strength that it has the characteristic emission spectrum in contrast to a FUor-type observed outburst. This source has been published in Contreras Peña et al. (2023), under the identifier SPICY 109331. This star makes an excellent test case for the other members of this group, with such features as a high-amplitude (3.28 mag) burst in $W1$, rising over a short time-frame of $\sim$ 2 yr, and becoming steadily bluer in its MIR colour, which is also seen in both FUors and V1647 Ori objects.

In addition to the sources identified by their MIR eruptive behaviour, two further LDE candidates were identified on the basis of outbursts observed between the UKIDSS UGPS (Lucas et al. 2017) NIR images (sources 362 and 1964). Both were identified by searching for bursts of at least 2 mag, wherein one UGPS epoch had a non-detection and the other had a minimum brightness of

Table 1. List of outbursting Cygnus-X members from Kryukova et al. (2014).

Source Number	RA (deg) J2000	Dec. (deg) J2000	$\Delta W1$ mag	$(W1-W2)_{\rm min}$ mag	Spectral index α	Time-scale Class	Outburst duration yr	Outburst rise time yr
12[a]	304.3677	+41.9736	2.004 ± 0.019	1.01	1.03	SDE	–	–
121[a,b]	305.5600	+37.4743	1.848 ± 0.038	1.73	1.61	SDE	–	–
185	305.8536	+37.5706	2.037 ± 0.07	3.05	−0.08	SDE	–	–
232	306.0890	+42.2683	1.692 ± 0.01	1.54	0.44	SDE	–	–
257[c]	306.1356	+37.8303	3.279 ± 0.013	1.65	1.23	LDE	24	2
294[a]	306.2141	+38.4203	2.524 ± 0.020	0.77	1.2	LDE	>30	7
333[b]	306.3550	+39.3400	2.055 ± 0.011	1.33	0.4	SDE	–	–
352[a]	306.4325	+38.1869	1.795 ± 0.020	2.82	1.52	SDE	–	–
362[d]	306.4640	+39.3760	2.402 ± 0.023	1.86	0.58	LDE	>10	?
387[a]	306.5333	+41.6357	2.437 ± 0.097	1.97	0.27	SDE	–	–
397	306.5526	+39.2783	2.262 ± 0.020	2.414	1.14	IDE	7–10	> 3
441	306.6371	+37.7786	1.674 ± 0.010	1.55	0.44	SDE	–	–
456	306.6672	+40.0418	0.978 ± 0.016	0.7	0.16	SDE	–	–
591	306.9916	+40.1975	2.354 ± 0.069	1.664	0.72	LDE	>30	2
625	307.0390	+40.1518	3.371 ± 0.031	1.32	0.2	IDE	4	<1
658[b]	307.1304	+41.8473	1.749 ± 0.011	1.26	0.27	IDE	5	≈1
769	307.4425	+39.2864	2.817 ± 0.050	1.95	0.66	SDE	–	–
812	307.5106	+40.3149	3.571 ± 0.046	1.93	1.54	IDE	6	<0.6
880	307.7106	+41.2442	2.634 ± 0.030	1.27	0.22	LDE	>10	?
912	307.7863	+40.0635	2.860 ± 0.036	2.732	0.88	LDE	>30	5
1017	308.0107	+40.3108	2.313 ± 0.165	2.39	1.14	IDE	6	≈1.5
1048	308.0877	+41.1318	3.981 ± 0.511	1.733	1.7	LDE	>30	7
1475	309.0957	+39.6769	2.210 ± 0.053	2.81	1.19	LDE	>30	1
1562[b]	309.3483	+42.2458	3.081 ± 0.062	2.49	1.01	IDE	3	<1
1626	309.5138	+42.5483	3.081 ± 0.008	1.16	0.09	SDE	–	–
1738	309.8197	+42.2693	2.401 ± 0.027	2.49	−0.05	Amb	?	?
1769[a,b]	309.9753	+42.0143	2.878 ± 0.008	2.27	1.15	Amb	?	?
1884	310.3783	+41.9181	1.438 ± 0.01	0.569	1.77	IDE	5.5	3
1945	310.6990	+42.7017	3.26 ± 0.041	1.961	0.77	LDE	10	3
1964[d]	310.8678	+42.8167	0.767 ± 0.007	1.517	0.82	LDE	>10	?
1991[a]	310.9918	+42.8032	3.035 ± 0.056	2.827	0.96	LDE	9?	7
1999	311.0531	+41.6165	4.606 ± 0.158	2.35	0.96	IDE	8	1.8
2003	311.0754	+41.6140	5.089 ± 0.017	1.67	1.01	Amb	?	?

Notes. LDE: long-duration eruptive sources with fast-rising FUor-type morphology and/or with outburst duration > 10 yr. IDE: intermediate-duration events with a duration between 2 and 10 yr. SDE: short-duration events including stochastic and quasi-periodic eruptive sources. Amb: ongoing outburst with ambitious duration.
[a]*The Spitzer* detection is a blend between two detectable sources in UGPS.
[b]Source has a light-curve morphology that is hard to be certain of an accretion-driven outburst.
[c]Source 257 is included in Contreras Peña et al. (2023).
[d]Sources previously found by the two-epoch UPGS photometry.

15 mag (2 mag above the lower limit of the survey). In each case, the lower limit for the non-detection was calculated for the relevant UGPS image, using the `ImageDepth` tool within the `Photutils` package (Bradley et al. 2021) (lower limits being 16.9 mag, and 17.0 mag for sources 362 and 1964, respectively). The post-outburst light curves are displayed in Fig. 2, both of which display the traditional fading behaviour of post-outburst FUors.

A second group within the LDEs are stars with extended rising times (greater than 3 yr) before reaching their photometric maxima, these are Sources 912, 1048, and 1991 in Fig. 3 (as well as Source 880 in Fig. B1). It is worth noting that sources 880 and 912 do seem to have faded from earlier observations, so there is a chance that these two systems may be'dippers'. These slow-rising infrared outbursts have been observed infrequently before (albeit prior to a higher amplitude outburst), such as the FUor *Gaia*17bpi (Hillenbrand et al. 2018), SSTgbs J21470601+4739394 (Ashraf et al. 2024), and VVVv721 (Contreras Peña et al. 2017a, b). This may suggest that the trigger for the outburst is driven by MRI (see Cleaver, Hartmann & Bae (2023) for simulations of the low-power Gaia17bpi-like FUor outbursts). Outbursts with rising times of the order of a decade (as seen here) are predicted in the flyby-triggered models of Borchert et al. (2022a), whose authors related these to outbursts of lower accretion rate, but feeding from a reservoir of material at a larger rotation radius, of the order of 40–50 au.

It is worth considering, however, the chance that these stars may not be eruptive at all, and are instead exhibiting behaviour that is analogous to long duration 'dippers' such as RW Aur (see Bozhinova et al. 2016). These long-duration variables are traditionally detected from the fading event (which can take up to a couple of years to reach minima), rather than the return to the star's normal baseline luminosity. These events typically result in the star becoming redder, and thus they would demonstrate blueing when increasing in brightness, as we might be seeing for our long-duration rising YSOs (for more information on this see Bouvier et al. 2013; Covey et al. 2021, and references therein). This behaviour is not entirely the case for UX Ori-type fades, which are likely caused by re-emission of stellar radiation from disc scattering, and thus show both reddening and blueing events when fading (see Herbst & Shevchenko

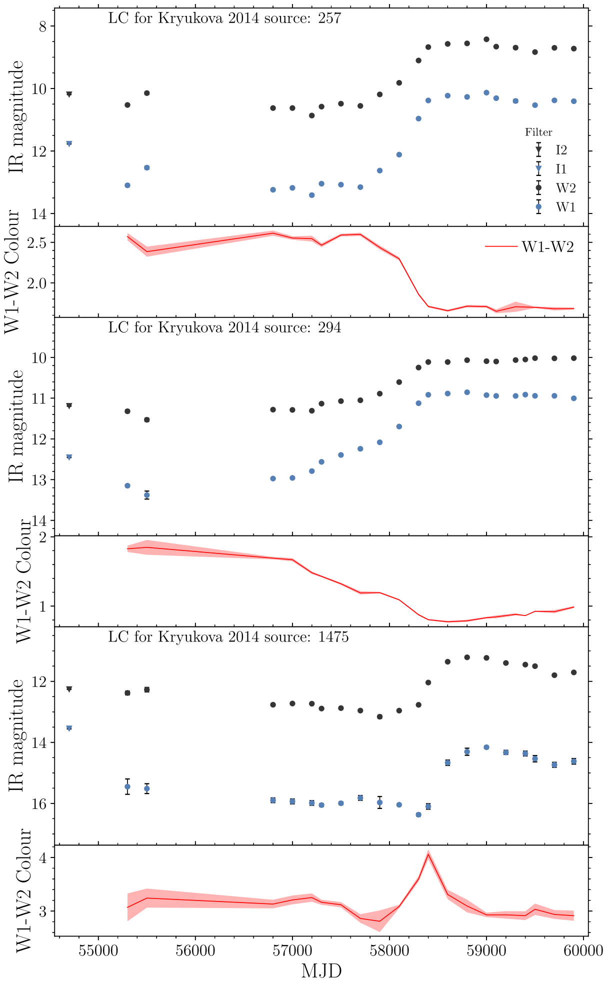

Figure 1. NEOWISE $W1$ and $W2$ light curves for three of the candidate EVs with FUor type light-curve morphologies. Each plot also contains a $W1-W2$ colour indicator (red line), with the error included as the pink-shaded region.

1999, for more details). We still prefer the eruptive classification for these sources owing to the higher observed amplitudes, and longer durations than the previously observed 'dippers'.

3.1.2 Intermediate duration eruptive YSOs

We identify eight stars in this sample with outbursts that are within the 2 to 10 yr boundary we set for the 'Intermediate-Duration Eruptive' (IDE) group. Of these, three targets (Sources 812, 1884, and 1999) have morphologies that resemble a FUor-type event (see Fig. 4), but are shorter than the >20-yr time-scales expected for FUors and are similar in morphology (if not amplitude) to VVV1636-4744 and L222_4 from Guo et al. (2024a). The two stars from Guo et al's sample have similar rise times (∼500 d) and NIR amplitudes of 4 and 6 mag respectively, but have differing spectral characteristics. L222_4 presents a typical red, absorption spectrum, typical of FUors, whereas VVV1636-4744 has an emission-line-dominated spectrum, more like EX Lup. Two further IDEs have completed outbursts (Sources 397 and 1017, Fig. C1). The final three IDEs (Sources 625, 658, and 1562, in Fig. C2) have a multipeaked shape to their light curves that do not resemble those of FUors.

Of the stars that resemble shorter duration FUors, we found some key differences between each star. For example, Source 812 displays

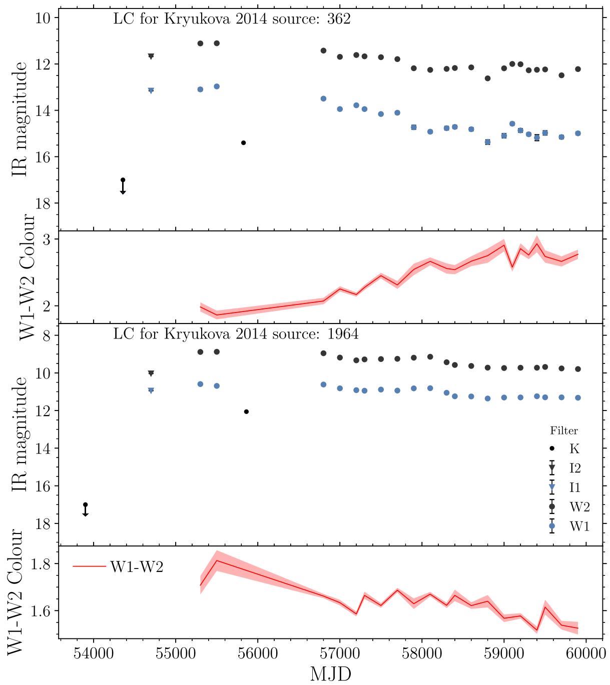

Figure 2. NEOWISE $W1$ and $W2$ light curves for the two LDE candidates identified with UGPS photometry. The arrows represent the upper limits of UGPS for each field.

at least 5 yr of a gradual increase in luminosity, before a very short (<6 months) outburst. This behaviour is similar to FUors like Gaia17bpi (with the two-stage initial outburst) as discussed earlier. Source 1999 has the second largest outburst in the sample but displays a much steeper decay slope than the three stars mentioned previously, indicative of a shorter outburst duration than most classical FUors, but longer than classical EXors (estimated at ≈8 yr). Finally, Source 1884 has the second lowest amplitude of the stars in this group at 1.44 mag (with a gradient of ≈ 0.36 mag yr^{-1}), but this is combined with the bluest quiescent $W1-W2$ colour (between 1.11 and 0.56 mag). Given the range in spectra seen in Guo et al. (2024a), acquiring NIR spectra for these three sources is essential in ascertaining the nature of the outbursts we have observed.

3.1.3 YSOs with short-duration outbursts

In total, there are 11 sources in this category, with the duration of outbursts less than 2 yr. Among them, seven stars have multiple bursts (four of these are semiregular, see Fig. 5) and four others only have a single burst. The rest of the light curves are shown in Figs 6 and B2. There are no clear trends within this group, with a broad spread in amplitude, burst duration and colour behaviour. There are several sources with multiple outburst-like events of quasi-periodic or aperiodic nature in this group, which are of a more uncertain classification. It could be assumed that occultation from circumstellar material (as in many 'dippers') would be periodic, and thus rule out the option for our repeating YSOs, but variation from circumbinary discs (as in KH 15D Arulanantham et al. 2016), as well as from misaligned or warped disc components (see Rodriguez et al. 2017; Davies 2019), can deliver aperiodic extinction driven variation in YSOs. In the optical regime, a large proportion of dippers found are aperiodic (see Capistrant et al. 2022), although the stars in those authors' samples were largely of a lower amplitude,

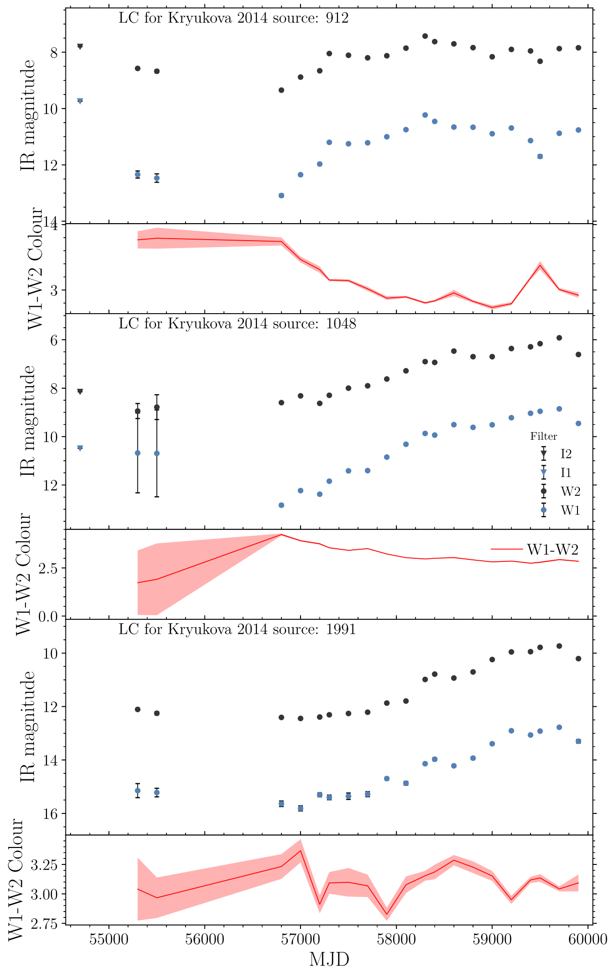

Figure 3. NEOWISE $W1$ and $W2$ light curves for three of the candidate EVs with longer duration rise times. Each plot also contains a $W1-W2$ colour indicator (red line), with the error included as the pink-shaded region.

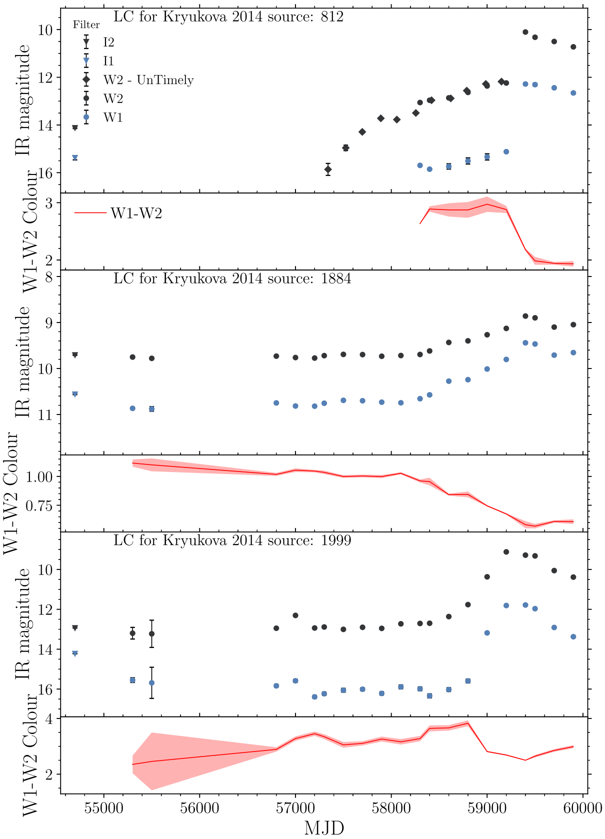

Figure 4. NEOWISE $W1$ and $W2$ light curves for three of the candidate EVs with shorter duration, FUor-like outbursts. Each plot also contains a $W1-W2$ colour indicator (red line), with the error included as the pink-shaded region. Source 812 also contains W2 data from the UnTimely catalogue (Meisner et al. 2023).

and bluer colour than ours, and had access to a much shorter time baseline that NEOWISE is not sensitive to. On the whole the morphologies of our repeating events (largely symmetrical) more closely resemble the short-term accretion-driven variations seen on many YSOs in the NIR, albeit at a higher amplitude. Similar behaviour was identified for a small number of YSOs in Wolk et al. (2018), which were also MIR-detected sources, although their YSOs were of lower amplitude, and displayed no colour change over time.

Some sources of note in this selection are discussed as following:

(i) Source 12 has four aperiodic outbursts with > 1 mag in $W2$-band amplitude. Unlike a typical EXor, Source 12 has redder-when-brighter colours, although given the large spectral index (1.03) this could be a result of reprocessing of more of the accretion luminosity into the MIR.

(ii) Source 185 has four quasi-periodic outbursts that each last for ~ 500 d (one of which is ongoing). We do not perceive the star to be a'dipper' because of the irregularity of the bursts (which could not be reliably fitted by normal period-finding routines), which would normally – although not guaranteed to – be periodic if caused by extinction from orbiting material. There is a chance that this object might represent contamination from an evolved star (such as a long-period variable), although these stars' MIR light curves are usually more regular than seen here.

(iii) Source 232 has a recent outburst, in addition to the one previously identified in the UGPS survey (included within Lucas et al. 2017). We will discuss it in more detail in Section 3.1.4.

(iv) Source 333 is of note from an additional long-duration outburst of 1.55 mag in $W1$, which has been ongoing since April 2019, although it reached its peak after ~ 600 d. This burst was accompanied by a small reduction in the $W1-W2$ colour, which was 2.13 at the start of the burst but fell to 1.50 at the maxima, and it continued to fall after the photometric maxima.

(v) Source 1626 (Fig. 6, bottom panel) has the largest single outburst amongst the short-duration sources at 2.37 mag in $W1$, which combines with a slight blueing $W1-W2$ colour of 0.28. The single large burst lasts only for ~ 500 d, all of which are indicative of an EXor-type eruption.

3.1.4 *Source 232*

Source 232, also known as GPSV28 (Contreras Peña et al. 2014) and IRAS 20226+4206, was observed to have probable outburst in December 2008 with $\Delta K_s = 1.0$ mag, originally detected by the UGPS survey (included as Source 463 in Lucas et al. (2017)), the amplitude increases to $\Delta K_s = 1.56$ mag when including 2MASS photometry. Additionally, it has two spectroscopic follow-up observations using Gemini/NIFS (2015) and Subaru/IRCS (2017). These spectra are shown in Fig. 7, which were acquired ∼4 and ∼6 yr after the previous outburst. The spectra show notable differences in the

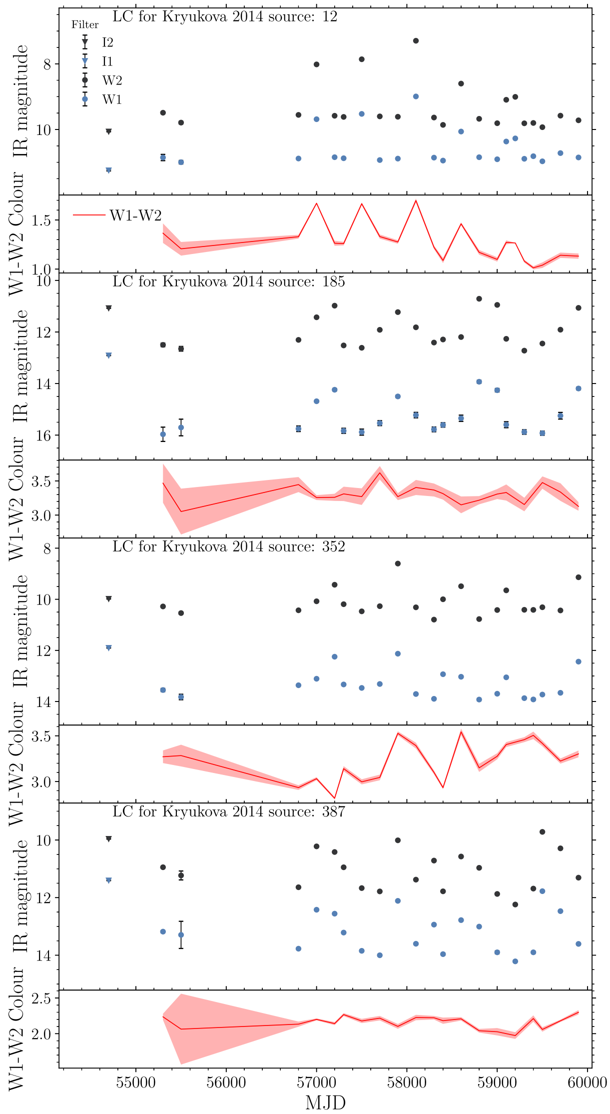

Figure 5. NEOWISE $W1$ and $W2$ light curves for the four semiregular repeating short-duration outbursts.

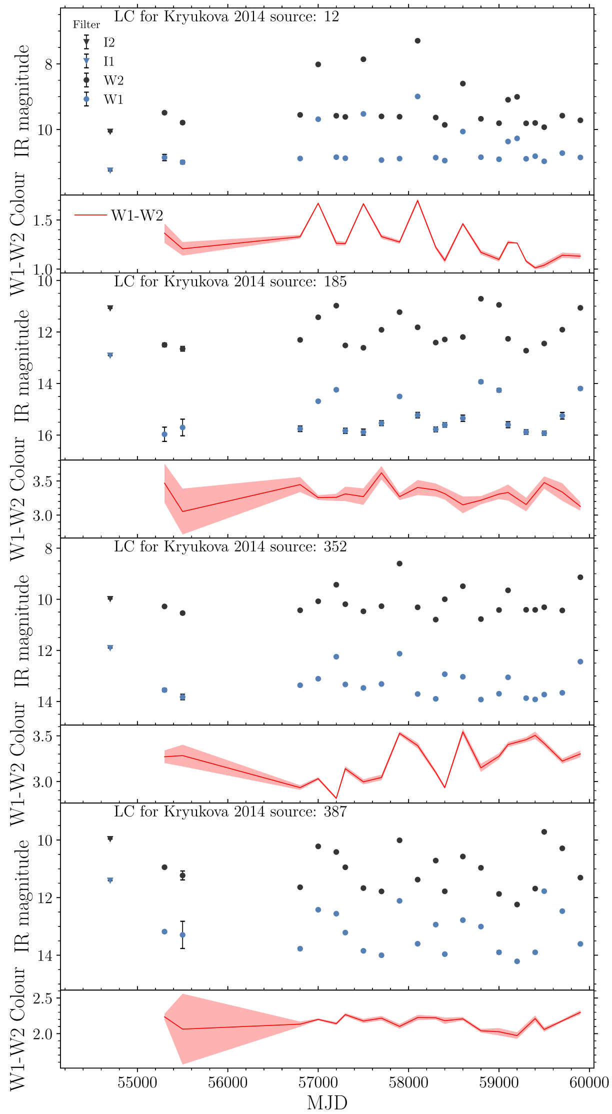

Figure 6. NEOWISE $W1$ and $W2$ light curves for four of the short-duration outbursts that have only one or two eruptive events.

emission line ratios, wherein the 2015 spectrum has more prominent H_2 lines (S(1) and S(0)) than H I, and a clear Na I doublet. The implication is that flux is a combination of the stellar photosphere, the inner accretion disc and outflows (traced by H_2). By the 2017 the spectrum is dominated by the Brγ emission line, with a 3.98$\pm$0.61 Å (from -1.98 ± 0.58 to -5.95 ± 0.2 Å) increase in equivalent width from the previous spectrum. Considering that this change implies an increase in the accretion rate, we speculate that a higher proportion of the observed flux is from the hot inner accretion disc, hence why emission lines associated with the accretion streams (Na I) are now significantly veiled by the continuum. Whilst the initial outburst of Source 232 was not fully captured by the *WISE* light curves, a second burst ($\Delta W1 = 1.4$ mag) was observed between 2021 and 2022, making clear that this star has EXor-like behaviour.

3.1.5 Eruptive YSOs with ambiguous outburst durations

The final three stars in this sample have ongoing outbursts, that are yet to reach the plateau, making it a challenge to determine a

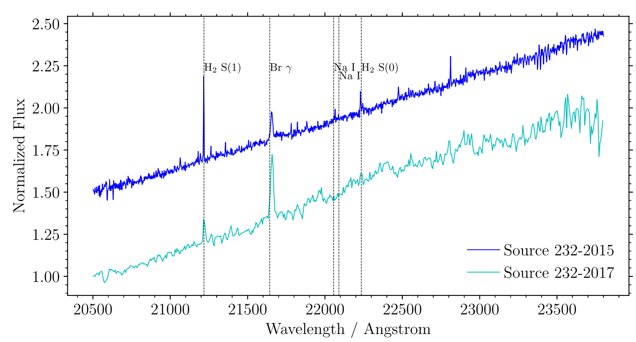

Figure 7. K and K' bandpass spectra for Source 232, taken in 2015 and 2017. Note the absence of lines from sodium in the 2017 spectrum, normally seen as a tracer of the accretion stream.

Table 2. 35 EV candidates found in SPICY with amplitude >1 mag.

SPICY ID	RA (deg) J2000	Dec. (deg) J2000	$\Delta W1$ mag	$(W1-W2)_{min}$ mag	Colour change (when brighter)	SED class
107 699	304.0523	+39.0873	1.025 ± 0.010	0.321	Redder	Class II
107 742	304.1969	+39.3892	1.054 ± 0.010	1.338	Bluer	Class II
107 855	304.3484	+39.3052	0.969 ± 0.008	0.550	No Change	Class II
108 504	305.3081	+38.9968	1.125 ± 0.013	0.441	Redder	Class II
108 553	305.3903	+40.8526	0.855 ± 0.017	0.698	Redder	Class II
108835[a]	305.7091	+40.5112	1.338 ± 0.046	0.786	Bluer	Class II
109 025	305.9034	+39.5591	0.875 ± 0.006	0.103	Redder	Class III
109259[a]	306.1053	+42.4036	1.233 ± 0.014	1.091	Bluer	Class II
109 392	306.1617	+38.5000	1.904 ± 0.015	0.332	Redder	Class II
109 705	306.4289	+38.5806	4.121 ± 0.021	1.171	Bluer	FS
109 973	306.6403	+39.6054	0.817 ± 0.021	0.345	Redder	Class II
110521[a]	307.0781	+39.4852	0.836 ± 0.007	0.157	Redder	Class II
110 601	307.1598	+38.8962	0.931 ± 0.010	0.416	Redder	Class III
110 991	307.4678	+40.4054	1.315 ± 0.008	0.713	Redder	Class II
111 048	307.5187	+40.3839	1.677 ± 0.011	0.025	Redder	Class II
111336[a]	307.7453	+40.5380	1.522 ± 0.036	−0.124	Redder	Class II
111413[a]	307.7927	+40.4144	1.165 ± 0.023	0.443	Redder	FS
111739[a]	307.9553	+38.9405	1.810 ± 0.067	1.346	Bluer	?
111 836	307.9984	+41.0660	1.125 ± 0.014	0.821	Redder	Class II
111 892	308.0221	+42.8133	0.876 ± 0.008	1.050	Varied	FS
112 458	308.2766	+40.7189	0.616 ± 0.057	−0.420	Redder	Class II
112 533	308.3147	+41.0470	1.561 ± 0.018	0.007	Redder	Class II
112 884	308.4971	+41.4482	0.614 ± 0.011	0.180	Redder	Class II
112979[a]	308.5504	+40.7098	1.201 ± 0.006	0.442	Redder	Class II
113094[a]	308.6131	+42.2315	1.672 ± 0.001	0.902	Bluer	Class II
113 145	308.6433	+41.1734	1.489 ± 0.015	0.643	Redder	Class II
113 564	308.9150	+41.8482	1.550 ± 0.016	0.609	Varied	Class II
113803[a]	309.0589	+41.1173	0.904 ± 0.009	0.166	Redder	Class III
113865[a]	309.0924	+42.4434	1.043 ± 0.049	−0.100	Varied	FS
113 929	309.1289	+39.6458	0.940 ± 0.005	0.441	Redder	Class II
114 037	309.1980	+42.6153	1.001 ± 0.051	−0.018	Varied	Class II
114471[a]	309.5422	+42.2826	1.371 ± 0.015	0.417	Bluer	Class II
114 590	309.6542	+42.5540	1.603 ± 0.034	0.542	Redder	FS
115 546	310.4321	+39.6725	0.662 ± 0.023	0.732	Redder	FS
115613[a]	310.5619	+39.7890	1.158 ± 0.010	0.777	No Change	FS

Notes. The colour behaviour column notes how the $W1-W2$ colour changes during the eruptive portions of the light curve: Bluer means the source is bluer-when-brighter (much like traditional EXors), Redder indicates redder-when-brighter behaviour, and 'Varied' notes stars whose colour behaviour changes over the total duration of the light curve. YSOs with $W1$ amplitudes under 1 mag have $\Delta W2 > 1$ mag. Sources marked with '[a]' indicate that the YSO has a light-curve morphology that is hard to be certain of an accretion driven outburst.

likely outburst duration (See Fig. C3 for light curves). Source 2003 is characterized by a large amplitude, 5.1 mag in W1, and colour change of over 1 mag to the blue in $W1-W2$ during the burst, both of which are common among FUor-type stars. With the outburst being unfinished, there is a possibility of it being one of the largest MIR outbursts yet detected for a FUor.

The remaining two stars in the group, sources 1738 and 1769, display similar long-term trends. Each star's light curve contains a small, short-term increase in brightness, before a visibly longer term outburst (ongoing). No other stars in the sample show such activity, and as yet the nature of the current outbursts is unknown.

3.2 Cygnus-X YSOs without [24] detections, from SPICY

Among the sample of the SPICY members, 402 stars have amplitudes of > 1 magnitude in either $W1$ or $W2$ band. We chose 1 mag as the threshold for inspection because MIR amplitudes are often a factor of 2 lower in amplitude than those seen in optical band-passes, and as such this corresponds to ≈2 mag, a little lower than the guidelines for an outburst as laid out by Fischer et al. (2022). The majority of the 402 stars showed single-epoch dipping events (likely extinction induced) or repeating redder-when-brighter'dipper' behaviour. We then manually selected 35 EV candidates (see Table 2), including seven FS sources, 24 Class II YSOs, and three Class III YSOs. An additional source is considered uncertain (it lacks photometry in multiple *Spitzer* bandpasses), although its average *WISE* colour ($W1-W2=1.66$) is comparable to the bluer Class I sources from Section 3.1.1.

Across the sample of EVs, 23/35 stars show the redder-when-brighter trend in their $W1-W2$ colour during outburst. Applying the outburst duration-based classifications defined in Section 3, we find 30 SDEs, one IDE, two LDEs, and two sources of ambiguous classification.

3.2.1 New FUor-type/long duration eruptive YSOs

The outburst detection code described in Section 2 located one star (SPICY 114590) with a shape comparable to that of an archetypal FUor (although the rise time is still on the longer scale, more similar to the VVV identified FUors), although it has a peak amplitude of

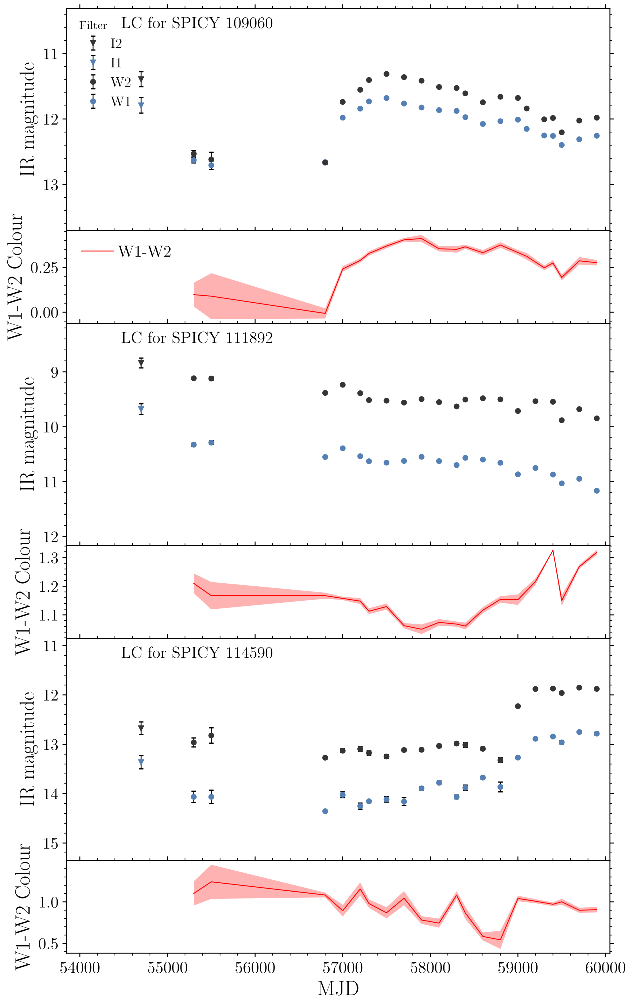

Figure 8. NEOWISE $W1$ and $W2$ light curves for three FUor candidates from the SPICY-selected Class II/FS sources.

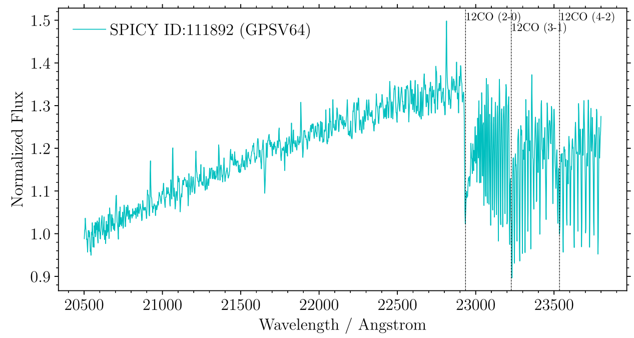

Figure 9. Gemini/NIFS spectrum for SPICY 111892. The spectrum is FUor-type, with a featureless red continuum and strong ^{12}CO absorption features.

< 2 mag (see Fig. 8). The MIR colour behaviour of SPICY 114590 is different to that seen in the FUor candidates in Section 3.1, as this object gets redder during the outburst. The low amplitude is not unexpected in the general sense, as it can be predicted by outburst models for YSOs with already enhanced accretion rates (see fig. 1 in Hillenbrand & Rodriguez 2022, with the caveat that this was for a sun-like star).

SPICY 111 892 has been previously identified as a candidate EV in UGPS by Contreras Peña (2015) and Lucas et al. (2017, as GPSV64). It displayed a 1.5 mag increase in K_s-band brightness between 2006 and 2009, which would be low for a FUor if this is the full amplitude of the event. However, the non-detection in earlier 2MASS images implies a longer rise time and a higher amplitude. The lower detection limit of the 2MASS K_s image in which SPICY 111 892 resides is calculated at 16.0 mag. This was calculated by running the `photutils` method called `ImageDepth`. This method takes the zero-point for the instrument, and a selection of magnitudes of stars in the image, and computes the lowest detectable flux for a given precision in sigma (quoted here are 3σ values) for a large number of randomly placed apertures. Thus, the total ΔK_s has a lower limit of 4.0 mag, with a rising time-scale of between ~1000 and ~4000 d. A follow-up spectrum was obtained in December 2014 (Fig. 9) with Gemini/NIFS, which shows the mostly featureless red continuum and CO bandheads often associated with FUor spectra (the emission line at 2.282 µm is likely spurious, as it had appeared in a large number of other YSOs in the same set of observations). See further examples of FUor-type spectra in Connelley & Reipurth (2018) and Guo et al. (2024a).

3.2.2 New EXor-like/short-duration eruptive YSOs

Of the 35 EV candidates in this group, 86 per cent (30) have short-duration outburst events, many of which are similar to EXor-like YSOs. In line with the known diversity of these systems, we observed significant variation in the light-curve morphologies, with differences in burst duration, amplitude, colour and repetition. We present four examples in Fig. 10 that illustrate the variety (the rest can be seen in Appendix D).

SPICY 113094 displays quasi-periodic behaviour at a roughly 550 d period,[3] with each burst of up to 1.6 mag and bluer colours during the photometric maxima. This is characteristic of stars such as SPICY 116 663 (Kuhn et al. 2021) and periodic outbursting candidates discovered in VVV (Guo et al. 2022), albeit with a longer period than most examples.

SPICY 110521 shows repeating burst behaviour, although without any clear periodicity, effectively ruling out periodic occultation by dust. With outbursts of over 1 mag and colours that redden with increases in luminosity, it is, however, unlike the typical behaviour of EXors Lorenzetti et al. (see 2012), wherein colours are often expected to become bluer during outbursts. The behaviour seen in SPICY 110 521 is commonly seen in this sample: 20 of 33 (60.6 per cent) short-duration (EXor-like) eruptive sources are redder in outburst.

SPICY 111336 also displays aperiodic, repetitive outbursts, but these are of differing amplitude, in contrast to many of the other repeating sources. The amplitudes in $\Delta W2$ range from ~ 0.7 to ~ 1.5 mag, although they are of a similar ~ 400 d duration (the duration is an upper limit owing to the wide sampling of NEOWISE). The range of amplitudes could also be a result of the sampling, with the peak of the outbursts being missed at several epochs, especially if the true period is less than 400 d.

The final EXor-like star to be discussed will be SPICY 112533, which is the most unusual star in this sample of later-stage YSOs. Seemingly there are two components to the light curve, with a potential long-term fading trend, which is separated into five detected outbursts each of between ~ 0.8 & 1.0 mag and ~ 1.0 & 2.0 mag in

[3]Fitted using the `astropy LombScargle` function.

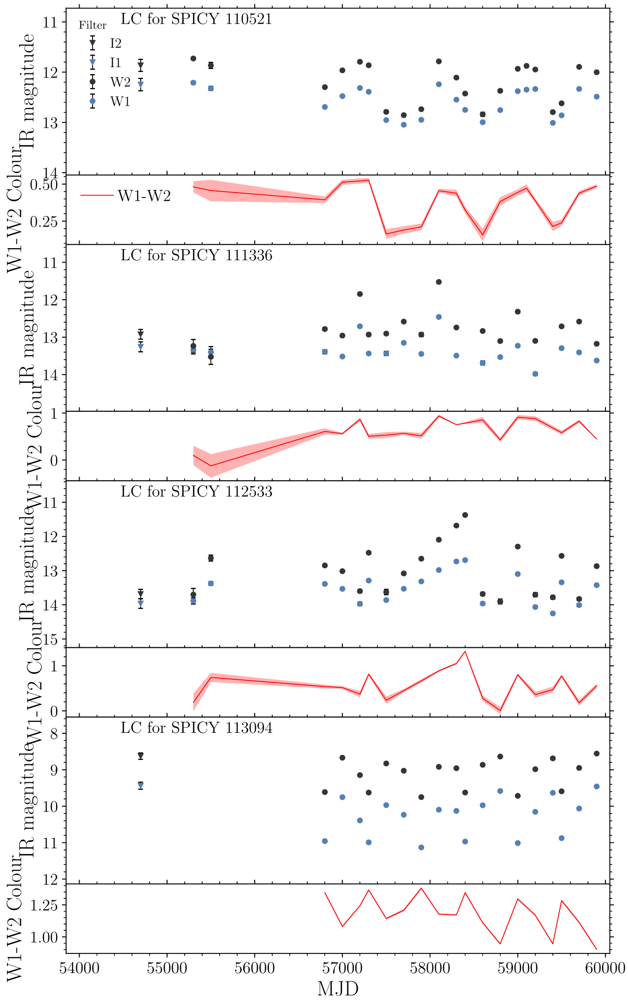

Figure 10. NEOWISE $W1$ and $W2$ light curves for four EXor candidate EVs. These are selected because they demonstrate a wide range of behaviours and outburst durations. Of particular note is Source 112533, which had periodic small outbursts after a much larger, long-duration event.

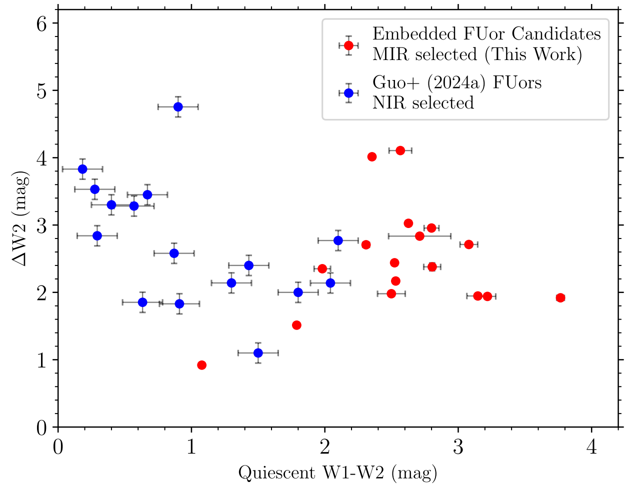

Figure 11. $W2$-band amplitude against quiescent $W1 - W2$ colour for EVs discussed in Section 3.1. The NIR-selected FUors are adopted from Guo et al. (2024a).

$W1$ & $W2$, respectively. Of additional note is the single outburst of at least 900 d (between 2016 and 2018) which bears little resemblance to other EXor-like bursts, owing to the comparatively short decay time-scale as compared to the rise time.

Overall the sample of short-term variables is slightly biased towards sources with repetitive outburst behaviour, as is the case for 60.6 per cent (20/33) of the sample. Whilst none of these are truly periodic, five of the stars display quasi-periodic bursts, with periods of over 400 d (the lowest that can be reliably identified with NEOWISE given the sampling).

4 DISCUSSION

4.1 Comparison of embedded FUor candidates with classical FUors

Given the comparatively low number of known FUor-like stars, our discovery of 13 (these being the stars with FUor-type light-curve morphologies or spectra) potential new candidates within a single SFR warrants additional investigation. Given that our main sample was of the most embedded EVs within Cygnus-X, comparing their MIR behaviour to that of FUors discovered via a 'traditional' optical outburst could reveal differences between the two populations.

Guo et al. (2024a) provided a selection of FUors discovered through analysis of the VVV NIR time series and further confirmed by follow-up spectroscopic observation. They found a negative correlation between the $\Delta W2$ and quiescent $W1 - W2$ colour (Fig. 11 – blue points), whereas this does not agree with the long-duration EVs in our sample (Fig. 11 – red points). The correlations were tested by performing Kendall τ tests on each sample, finding the NIR selected sources to have $\tau = -0.42$, compared to $\tau = 0$ for the MIR selected EVs from this work. Our EVs from Kryukova et al. (2014) seem to have no correlation between $\Delta W2$ and $W1 - W2$, although all still show the common bluer-when-brighter colour behaviour during the outburst, similar to FUors. The figure also places the slowly rising EVs amongst the FUor candidates, giving further weight to our hypothesis that these sources are YSOs that are building up to a FUor-type outburst (which may be optically detectable), in a similar vein to Gaia17bpi.

The reasoning for the break in the correlation of the colour/amplitude relation for the embedded sources is not yet fully clear, although a thicker envelope (and thus redder quiescent colours) might imply that we are seeing greater reprocessing of the accretion luminosity into the MIR, inflating the observed amplitude.

4.2 Less-than-certain short-duration YSO outbursts

Distinguishing short-duration eruptive events from dippers within our sample is an uncertain task, owing to the long cadence of the NEOWISE observation windows. The morphology of individual events can be hard to determine, and the colour behaviour during brightening can be impacted by numerous factors including inclination and the faint nature of some of our targets (see Section 4.4). Previous work on the MIR variability of YSOs with the *Spitzer* YSOVAR programme (Werner et al. 2004; Morales-Calderón et al. 2011) focused on variability with time-scales of weeks to a month (which would likely appear without a clear structure in NEOWISE). In Wolk et al. (2018), authors found an average amplitude of 0.21/0.13 mag in IRAC (Fazio et al. 2004) $I1$ and 0.17/0.13 mag in $I2$ for Class I/II sources in the star-forming region Serpens South ($I1$ and $I2$ are roughly analogous

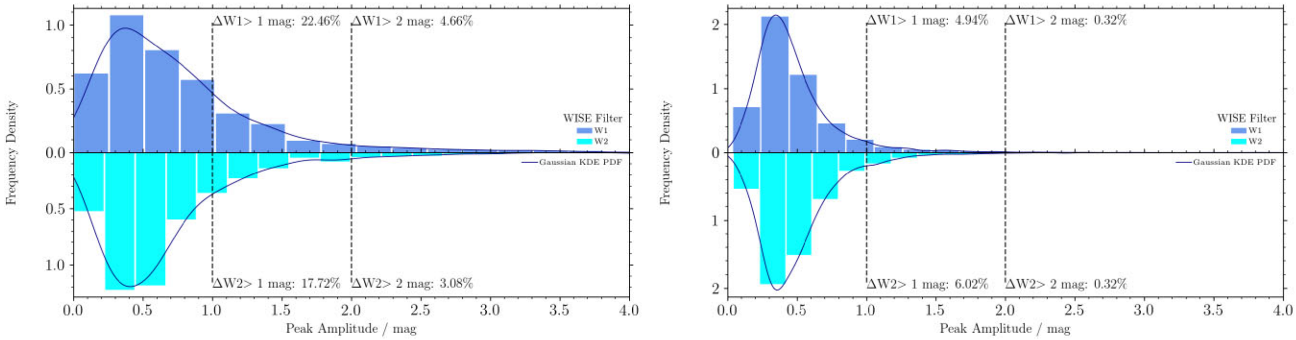

Figure 12. Histograms displaying peak amplitudes in $W1$ and $W2$ for both of the two samples discussed in Section 3. The left plot is the [24] detected sample, and the SPICY selected C2 and FS sources are in the right panel. Each individual histogram is presented with a probability distribution function, created by performing a Gaussian kernel density estimation.

$W1$ and $W2$). Notably, none of the YSOs in the Serpens South samples have an amplitude greater than 1 mag. In the Orion nebula, only 13 out of 2238 sources reached 1 mag in their $I1$ or $I2$ amplitudes on the time-scale of 2 weeks.

Our selection of stars with at least one bandpass with amplitudes of >1 mag was intended to remove the majority of stars with the type of short-term variance seen previously. It remains to be seen how successful this has been, with several (19) YSOs having light-curve morphologies which are far removed from those expected of eruptive stars (see marked ‘a’ YSOs in Tables 1 and 2). These stars not only carry the possibility of being dippers, but they could also belong to the loose grouping of ‘Protostellar Outbursts (Infrared)’, which was detailed in Fischer et al. (2022). These shorter duration events of around 1–2.5 mag in the NIR, would correspond to ∼0.6–1.5 mag in the *WISE* bandpasses (Contreras Peña et al., in preparation); a similar region to where many of our SDE’s that do not resemble EXors (or repeating EXors) reside. Follow-up spectroscopy of these stars may shed further light on to the causes of the observed variability, and thus determine if they are from a single, cohesive group. Accounting for these less-than-certain eruptions, we can say that we have identified 48 strong candidate EVs, with a further 20 uncertain.

4.3 Comparing the rates of eruptive behaviour between embedded and non-embedded sources

By having a control sample of known YSOs, we can compare both the detection rates and amplitudes of eruptive variability for our embedded YSOs to those of the less embedded or more evolved sources within Cygnus-X. The comparisons between the frequency density and amplitude for our samples are shown in Fig. 12, with embedded Class I sources in the left panel, and FS/Class II sources in the right. The embedded sources have a higher proportion of high-amplitude variables than the later stage sources, as 22.46 per cent of Class I YSOs (From the 24µm selected sample) have $\Delta W1 > 1$ mag whilst just 4.94 per cent FS/Class II YSOs (the SPICY sample) reach the same amplitude. We note that only a proportion of these variables are eruptive, with large numbers of dippers, short-term variables and stars on long-term fading trends. Nevertheless, the fading sources may well be eruptive YSOs, wherein a large outburst has happened before our observation window and we are now witnessing the post-outburst cooling phase

To test the significance of these results, we performed a Mann–Whitney U (MW-U) test, between both samples. Because the sample of FS/Class II sources is substantially larger than that of Class I sources, we performed the MW-U test on two equal-sized samples drawn from distributions defined by a Gaussian kernel density estimation (fitted to all four histograms in Fig. 12). Both of these routines are carried out in PYTHON, using the `gaussian_kde` routine in `scipy.stats`. This test produced an average p-value of 3.46 per cent over 10 000 iterations and thus provided moderately statistically significant evidence that these two samples were drawn from two different distributions.

From the perspective of YSO evolution, the above result is within expectation, as younger systems have a larger reservoir of material to accrete from. Massive discs with envelopes are also more likely to become unstable under gravity, especially when considering that flyby events are likely to be more common in younger (less bound) clusters. For further discussion of this idea, see Audard et al. (2014).

Given the potentially higher chance for outbursts, searching for EVs amongst younger systems specifically should result in a larger sample, especially of the rarer FU Ori-type objects. This falls into the long-held view that longer duration outbursts happen in younger systems (Hartmann & Kenyon 1996), given the long average length of FUor events. The differing morphologies among our long-duration outbursts also fit into the ideas of Quanz et al. (2007), which describe a possible evolutionary sequence for FUors, based upon their MIR features. The above point makes a strong case for follow-up spectroscopy at both near and MIR wavelengths.

To further investigate the relationship between outburst amplitude and age for YSOs, we compared the combined sample of YSOs on the basis of the 0.8–12 µm spectral index (α). Fig. 13 shows the proportion of high-amplitude variables increasing with α, noting the decrease in kurtosis for the later stage YSOs indicates that the distribution becomes more centrally dominant (and thus lower amplitude on average).

We can also examine the time-scales of the observed variability, i.e. the durations of individual variable events. For our sample, we wish to identify any relationship between outburst duration and evolutionary stage, and thus we separate our sample of stars with > 1 mag variability by the same spectral index groups as before. We use structure functions as an analogue to time-scale, as laid out in Sergison et al. (2020) and Lakeland & Naylor (2022), although similar tests for YSO variability were carried out in Findeisen, Cody & Hillenbrand (2015).

$$S(\tau) = \langle [m(t) - m(t+\tau)]^2 \rangle, \quad (5)$$

where S is the structure, τ is the time-scale between two points in a light curve, m is the apparent magnitude, and t is the modified Julian date of any given point in the light curve. This function produces a measure of correlation between each point in a light curve for a range

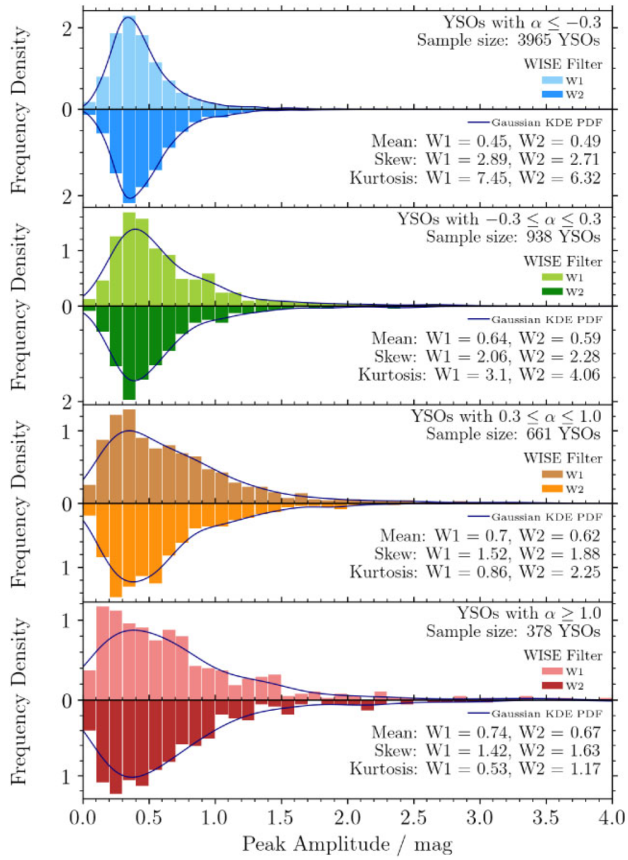

Figure 13. $W1$ and $W2$ amplitude histograms for the combined YSO sample, split by SED slope class (α).

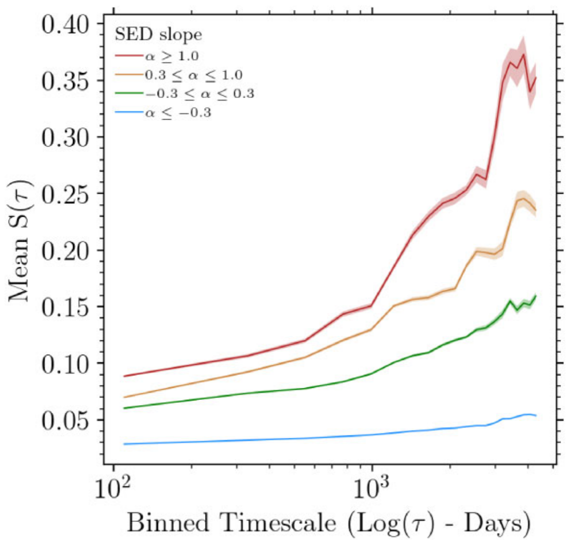

Figure 14. Structure functions across a range of time-scales for the combined YSO sample. Each point is the median structure in each time-scale bin, averaged for both $W1$ and $W2$. These are once again separated by the value of the α parameter for the SED slope.

of time baselines (we use 12 bins ranging from ∼100 d to ∼10 yr). In Fig. 14, we show that the signal is well correlated (S is low) at the shortest time-scales (here that is of the order of 3 months), and becomes less so as the time-scale increases (S is large). The implications here are that at shorter time-scales it is easier to predict the next measurement in the time series (i.e. is less variable), and gets progressively more challenging at longer time baselines. It is worth noting that we do not see the higher S values at the short time-scales that Lakeland & Naylor (2022) attributed to measurement error and short-term variability because our data from NEOWISE have been averaged at the shortest time baselines. We do see the same 'Knee' feature at large τ for 3 of the groups however, which those authors attributed to a combination of long-term linear trends or a maximum variability time-scale for YSOs.

From both of the above tests, it seems apparent that long-duration, high-amplitude variability is more common for more heavily embedded (likely younger) YSOs, as has been suggested previously (see Contreras Peña et al. 2024).

4.4 Outburst colour changes

Most outbursting YSOs are observed to be bluer during an outburst, when compared against their pre-outburst colour. Within the optical regime, the blueing is most prominent in EXors (see Lorenzetti et al. 2012; Szegedi-Elek et al. 2020), for which the significantly increased accretion luminosity of the innermost part of the system dominates over the flux contribution from the outer disc (during outburst). This remains true (albeit to a lesser extent) for most FUors and other long-duration eruptive systems. The effect is less studied in the MIR, where the flux contribution from the cooler parts of the disc is greater.We compared the $W2$ amplitudes with the SED class of the stars in our sample and a selection of long-duration eruptive YSOs, most of which were spectroscopically confirmed as FUors, from Guo et al. (2024a). Additionally, we investigated the colour change in $W1 - W2$, see Fig. 15. We have several broad findings:

(i) Our full sample, see the lower panel of Fig. 15, has a typical behaviour of becoming redder when brighter. In particular, we note that YSOs with [24] detections have larger changes in colour, having a median absolute colour change of 0.43 in $W1 - W2$, compared to 0.23 for the sources from SPICY.

(ii) We also note that the majority of our candidate FUors display the expected blueing during outbursts, in agreement with the long duration EV sample of Guo et al. (2024a) (see the upper panel of Fig. 15). The colours of our mid-IR-selected FUor candidates change less than the NIR-selected sources of those authors' sample however.

(iii) Our selection of Class II/FS YSOs (from SPICY) are preferentially redder when brighter, which might be attributed to the fainter $W2$ magnitudes of these stars (in quiescence); this sample has a median quiescent brightness of $W1 = 12.46$ mag, compared to 11.31 mag for the Class I sample. Given the logarithmic nature of the magnitude scale, a lower proportion of flux from enhanced accretion would be required to increase the magnitude of $W2$ than $W1$. The large YSO sample of Park et al. (2021a) (also using the NEOWISE time series) displayed a broad range of colour behaviours, similar to what we observe within our sample. Those authors attribute the behaviour to the interplay between accretion luminosity changes (bluer) as well as variable extinction from circumstellar material (redder), which can be moved during outburst.

5 SUMMARY

In this work, we have presented 68 potential candidate EV YSOs associated with the Cygnus X star-forming region, based on their decade-long MIR NEOWISE light curves.

In total, we discovered 14 eruptive sources that we believe to be FUor candidates, which can be seen in Table 3. Of these 14, 8

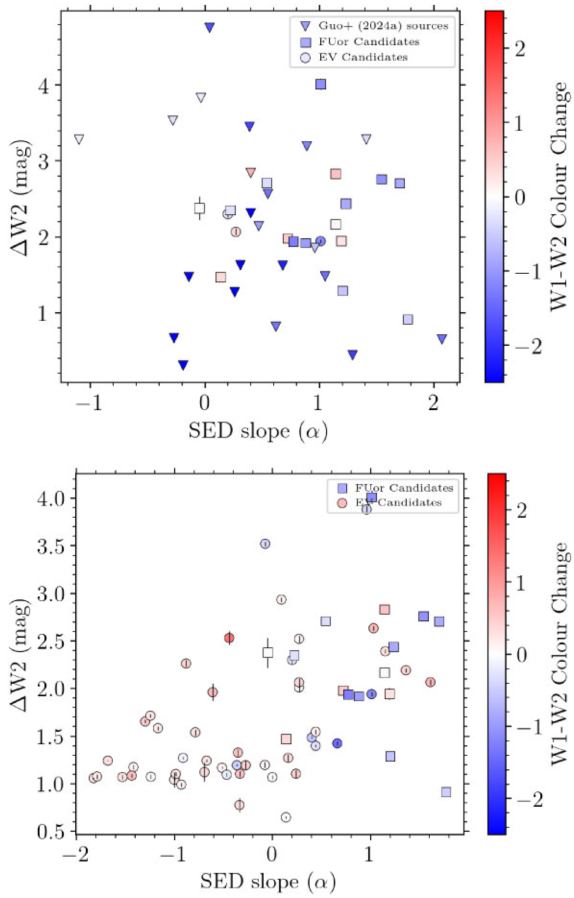

Figure 15. Top panel: $W2$-bandpass amplitudes for the stars in the sample with outbursts labelled as IDEs or LDEs (detected during outburst), against the pre-outburst SED slopes. The colour change during outburst is presented as the marker colour, with red points reddening during outburst and the opposite true for blue markers. White points represent stars with minimal colour change. Our sample of stars is represented by the circular and square points (for our uncertain and FUor candidates respectively). We include the NIR selected FUors (triangles) from Guo et al. (2024a) to compare our YSOs with those selected from large amplitudes in the K_s bandpass. The $\Delta W2$ values from that sample are based on lower limits for stars where there is no detection in $W2$. Bottom panel: similar plot for all the YSOs included in this work, regardless of outburst duration.

have light-curve morphologies similar to those of FUors or V1647 Ori-type stars. Three candidates show only a fading trend in their MIR light curves but have evidence for an initial rise in earlier NIR photometry. Two stars have extended brightening phases, comparable to V1515 Cyg. One final source has a currently ongoing outburst. In addition, six other sources are classified as plausible FUor candidates, with less clear light curves and more short-term variation.

We also locate a large number of YSOs with short-duration outbursts (some with EXor-like features) within both samples carried out, with 13 embedded Class I YSOs and 32 FS or Class II stars. Compared with more evolved systems, we detected significantly more high-amplitude (and eruptive) variables among the Class I YSOs (22.46 per cent). This is especially true for the FUor type EVs, of which we have identified up to 16 candidate members, and several have a less common, slow-rising character. Given the similarities between these objects and the pre-outburst light curves of several novel FUors, these 'slow-risers' might be further examples of FUors that outburst at earlier times in redder wavelengths.

Table 3. List of the FUor candidates from this work, both samples and all durations.

Source ID (this work)	Time-scale category	Amplitude ($W1$)	Colour change (when brighter)
	Likely candidates		
257	LDE	3.28	Bluer
294	LDE	2.52	Bluer
362	LDE	–[a]	Bluer
591	LDE	2.35	Bluer
812	IDE	3.57	Bluer
1048	LDE	3.98	Bluer
1475	LDE	2.81	Varied
1884	IDE	1.44	Bluer
1945	LDE	1.96	Bluer
1964	LDE	–[a]	Redder
1991	LDE	2.82	Bluer
1999	IDE	2.35	Bluer
2003	Amb	5.09	Bluer
111892	LDE	–[a]	Varied
	Potential candidates		
397	IDE	2.26	Bluer
880	LDE	2.63	Varied
912	LDE	2.86	Bluer
1017	IDE	2.31	Redder
1738	Amb	2.40	Bluer
114590	LDE	1.60	Redder

Notes. [a]These stars had their outbursts discovered with NIR data, so the $W1$ amplitudes are not included. Also note that the stars labelled as IDEs have their time-scales estimated via their initial fading period, and could still take longer than 10 yr to return to quiescence.

Given this potentially new population of eruptive young stars, follow-up observations are planned for those stars still at a state of high accretion rate and are thus bright in the NIR. This attempt may unveil any differences in accretion behaviour and disc/wind structure between the heavily embedded EVs and those sources selected via NIR/optical variability.

Finally, we note the increased incidence of high-amplitude variability for embedded YSOs (Class I), as compared to less embedded sources (FS and class II). We identified that the rate of variability of amplitudes that are >1 mag ranged from 2.9 times greater in $W1$, to 4.6 times greater in the $W2$ bandpass.

ACKNOWLEDGEMENTS

ZG is supported by the ANID FONDECYT Postdoctoral program No. 3220029. This work was funded by ANID, Millennium Science Initiative, AIM23-0001. PWL acknowledges support from the UK's Science and Technology Facilities CouncilST/Y000846/1. CM, PWL and NM recognize the computing infrastructure provided via STFC grant ST/R000905/1 at the University of Hertfordshire. CCP was supported by the National Research Foundation of Korea (NRF) grant funded by the Korean government (MEST) (no. 2019R1A6A1A10073437).

This publication makes use of data products from the Near-Earth Object Wide-field Infrared Survey Explorer (NEOWISE), which is a joint project of the Jet Propulsion Laboratory/California Institute of Technology and the University of Arizona. NEOWISE is funded by the National Aeronautics and Space Administration. This research has made use of the NASA/IPAC Infrared Science Archive, which is funded by the National Aeronautics and Space Administration and operated by the California Institute of Technology.

This work has made use of the University of Hertfordshire's high-performance computing facility (http://uhhpc.herts.ac.uk).

DATA AVAILABILITY

The *WISE* and *Spitzer* data underlying this article are publicly available at the IRSA server https://irsa.ipac.caltech.edu/Missions/wise.html. ALLWISE/NEOWISE light curves are available at http://star.herts.ac.uk/~cmorris/CygnusX_YSOs/. Reduced spectra are provided at http://star.herts.ac.uk/~cmorris/.

REFERENCES

Acosta-Pulido J. A. et al., 2007, AJ, 133, 2020
Arulanantham N. A. et al., 2016, AJ, 151, 90
Ashraf M., Jose J., Lee H.-G., Contreras Peña C., Herczeg G. J., Liu H., Johnstone D., Lee J.-E., 2024, MNRAS, 527, 11651
Aspin C., Briceno C., Downes J., Hernandez F., Rojas R., Nakano M., 2009, IAU Circ., 9079, 1
Audard M. et al., 2014, in Beuther H., Klessen R. S., Dullemond C. P., Henning T., eds, Protostars and Planets VI. Univ. Arizona Press, Tucson, AZ, p. 387
Barentsen G. et al., 2014, MNRAS, 444, 3230
Beerer I. M. et al., 2010, ApJ, 720, 679
Bell K. R., Lin D. N. C., 1994, ApJ, 427, 987
Benjamin R. A. et al., 2003, PASP, 115, 953
Borchert E. M. A., Price D. J., Pinte C., Cuello N., 2022a, MNRAS, 510, L37
Borchert E. M. A., Price D. J., Pinte C., Cuello N., 2022b, MNRAS, 517, 4436
Bourdarot G. et al., 2023, A&A, 676, A124
Bouvier J. et al., 2007, A&A, 463, 1017
Bouvier J., Grankin K., Ellerbroek L. E., Bouy H., Barrado D., 2013, A&A, 557, A77
Bozhinova I. et al., 2016, MNRAS, 463, 4459
Bradley L. et al., 2021, astropy/photutils: 1.2.0. Zenodo. Available at: https://doi.org/10.5281/zenodo.5525286
Briceño C. et al., 2004, ApJ, 606, L123
Capistrant B. K. et al., 2022, ApJS, 263, 14
Clarke C., Lodato G., Melnikov S. Y., Ibrahimov M. A., 2005, MNRAS, 361, 942
Cleaver J., Hartmann L., Bae J., 2023, MNRAS, 523, 5522
Connelley M. S., Reipurth B., 2018, ApJ, 861, 145
Contreras Peña C. E., 2015, PhD thesis, Univ. Hertfordshire
Contreras Peña C. et al., 2014, MNRAS, 439, 1829
Contreras Peña C. et al., 2017a, MNRAS, 465, 3011
Contreras Peña C. et al., 2017b, MNRAS, 465, 3039
Contreras Peña C., Johnstone D., Baek G., Herczeg G. J., Mairs S., Scholz A., Lee J.-E., Team T. J. T., 2020, MNRAS, 495, 3614
Contreras Peña C. et al., 2023, J. Korean Astron. Soc., 56, 253
Contreras Peña C., Lucas P. W., Guo Z., Smith L., 2024, MNRAS, 528, 1823
Covey K. R., Larson K. A., Herczeg G. J., Manara C. F., 2021, AJ, 161, 61
Cuello N. et al., 2019, MNRAS, 483, 4114
Davies C. L., 2019, MNRAS, 484, 1926
Drew J. E. et al., 2005, MNRAS, 362, 753
Fazio G. G. et al., 2004, ApJS, 154, 10
Findeisen K., Cody A. M., Hillenbrand L., 2015, ApJ, 798, 89
Fischer W. J. et al., 2017, ApJ, 840, 69
Fischer W. J., Hillenbrand L. A., Herczeg G. J., Johnstone D., Kóspál Á., Dunham M. M., 2022, in Inutsuka S., Aikawa Y., Muto T., Tomida K., Tamura M., eds, ASP Conf. Seri., Vol. 534, Protostars and Planets VII. Astron. Soc. Pac., San Francisco
Gaia Collaboration 2023, A&A, 674, A1
Greene T. P., Lada C. J., 1996, AJ, 112, 2184
Guo Z. et al., 2020, MNRAS, 492, 294
Guo Z. et al., 2021, MNRAS, 504, 830
Guo Z. et al., 2022, MNRAS, 513, 1015
Guo Z. et al., 2024a, MNRAS, 528, 1769
Guo Z. et al., 2024b, MNRAS, 529, L115
Hartmann L., Kenyon S. J., 1996, ARA&A, 34, 207
Hartmann L., Zhu Z., Calvet N., 2011, preprint (arXiv:1106.3343)
Herbst W., Shevchenko V. S., 1999, AJ, 118, 1043
Hillenbrand L. A., Rodriguez A. C., 2022, Res. Notes Am. Astron. Soc., 6, 6
Hillenbrand L. A. et al., 2018, ApJ, 869, 146
Hora J. et al., 2007, A Spitzer Legacy Survey of the Cygnus-X Complex. Spitzer Proposal ID #40184
Kiwy F., 2022, Astrophysics Source Code Library, record ascl:2211.005
Kobayashi N. et al., 2000, in Iye M., Moorwood A. F., eds, SPIE Conf. Ser. Vol. 4008, Optical and IR Telescope Instrumentation and Detectors. SPIE, Bellingham, p. 1056
Koenig X. P., Leisawitz D. T., 2014, ApJ, 791, 131
Kratter K., Lodato G., 2016, ARA&A, 54, 271
Kryukova E. et al., 2014, AJ, 148, 11
Kuhn M. A., de Souza R. S., Krone-Martins A., Castro-Ginard A., Ishida E. E. O., Povich M. S., Hillenbrand L. A., COIN Collaboration, 2021, ApJS, 254, 33
Kuhn M. A., Benjamin R. A., Ishida E. E. O., de Souza R. S., Peloton J., Veneri M. D., 2023, Res. Notes Am. Astron. Soc., 7, 57
Lakeland B. S., Naylor T., 2022, MNRAS, 514, 2736
Li J., Wang T., 2024, MNRAS, 532, 2683
Liu H. et al., 2022, ApJ, 936, 152
Lorenzetti D. et al., 2012, ApJ, 749, 188
Lucas P. W. et al., 2008, MNRAS, 391, 136
Lucas P. W. et al., 2017, MNRAS, 472, 2990
Lucas P. W. et al., 2020, MNRAS, 499, 1805
Lucas P. W. et al., 2024, MNRAS, 528, 1789
McGregor P. J. et al., 2003, in Iye M., Moorwood A. F. M., eds, SPIE Conf. Ser. Vol. 4841, Instrument Design and Performance for Optical/Infrared Ground-based Telescopes. SPIE, Bellingham,p. 1581
Mainzer A. et al., 2014, ApJ, 792, 30
Meisner A. M., Lang D., Schlegel D. J., 2018, AJ, 156, 69
Meisner A. M., Caselden D., Schlafly E. F., Kiwy F., 2023, AJ, 165, 36
Minniti D. et al., 2010, New Astron., 15, 433
Morales-Calderón M. et al., 2011, ApJ, 733, 50
Nayakshin S., Elbakyan V., 2024, MNRAS, 528, 2182
Nayakshin S., Cruz Sáenz de Miera F., Kóspál Á., Ćalović A., Eislöffel J., Lin D. N. C., 2024, MNRAS, 530, 1749
Ninan J. P., Ojha D. K., Bhatt B. C., Ghosh S. K., Mohan V., Mallick K. K., Tamura M., Henning T., 2013, ApJ, 778, 116
Park W. et al., 2021a, ApJ, 920, 132
Park S. et al., 2021b, ApJ, 923, 171
Park S. et al., 2022, ApJ, 941, 165
Park G. et al., 2024, AJ, 168, 122
Quanz S. P., Henning T., Bouwman J., van Boekel R., Juhász A., Linz H., Pontoppidan K. M., Lahuis F., 2007, ApJ, 668, 359
Rodriguez J. E. et al., 2017, ApJ, 848, 97
Rygl K. et al., 2012, A&A, 539, A79
Schlafly E. F. et al., 2018, ApJS, 234, 39
Scholz A., Froebrich D., Wood K., 2013, MNRAS, 430, 2910
Sergison D. J., Naylor T., Littlefair S. P., Bell C. P. M., Williams C. D. H., 2020, MNRAS, 491, 5035
Skrutskie M. F. et al., 2006, AJ, 131, 1163
Stauffer J. et al., 2014, AJ, 147, 83
Szegedi-Elek E. et al., 2020, ApJ, 899, 130
Tokunaga A. T. et al., 1998, in Fowler A. M.ed., SPIE Conf. Ser. Vol. 3354, Infrared Astronomical Instrumentation. SPIE, Bellingham, p. 512
Tran V., De K., Hillenbrand L., 2024, MNRAS, 530, 2076
Venuti L. et al., 2019, A&A, 632, A46
Vorobyov E. I., Basu S., 2010, ApJ, 719, 1896
Werner M. W. et al., 2004, ApJS, 154, 1
Whitney B. et al., 2011, in American Astronomical Society Meeting Abstracts #217. p. 241.16
Wolk S. J. et al., 2018, AJ, 155, 99
Wright E. L. et al., 2010, AJ, 140, 1868
Zhu Z., Hartmann L., Gammie C., McKinney J. C., 2009, ApJ, 701, 620

SUPPORTING INFORMATION

Supplementary data are available at *MNRAS* online.

NEOWISE_CygX_SPICY_EX_4.pdf
NEOWISE_CygX_SPICY_EX_5.pdf
NEOWISE_CygX_SPICY_EX_6.pdf
NEOWISE_CygX_SPICY_EX_7.pdf

Please note: Oxford University Press is not responsible for the content or functionality of any supporting materials supplied by the authors. Any queries (other than missing material) should be directed to the corresponding author for the article.

APPENDIX A: OUTBURST TIME-SCALE FITS WITH EMCEE

The plots below demonstrate some of the results of fitting a characteristic FUor-type shape to a NEOWISE light curve. As mentioned in the text (Section 2.1) we use EMCEE to fit three light-curve components (representing the start of the outburst, the main rising slope, and the post-outburst linear decay) with five free parameters. Candidates were marked for further investigation if the reduced mean square error (RMSE) was less than 0.15. This value has been selected initially because it allows the code to recover all the stars in the sample that visual inspection identified as FUor candidates, with reasonably typical light curves. The code does not recover the stars with consistent (and fairly slow) rising slopes, such as Source 1048. In a sample of stars of this size, our fitting technique is of questionable utility, however, it will be of use when examining larger populations for which visual inspection would be inefficient.

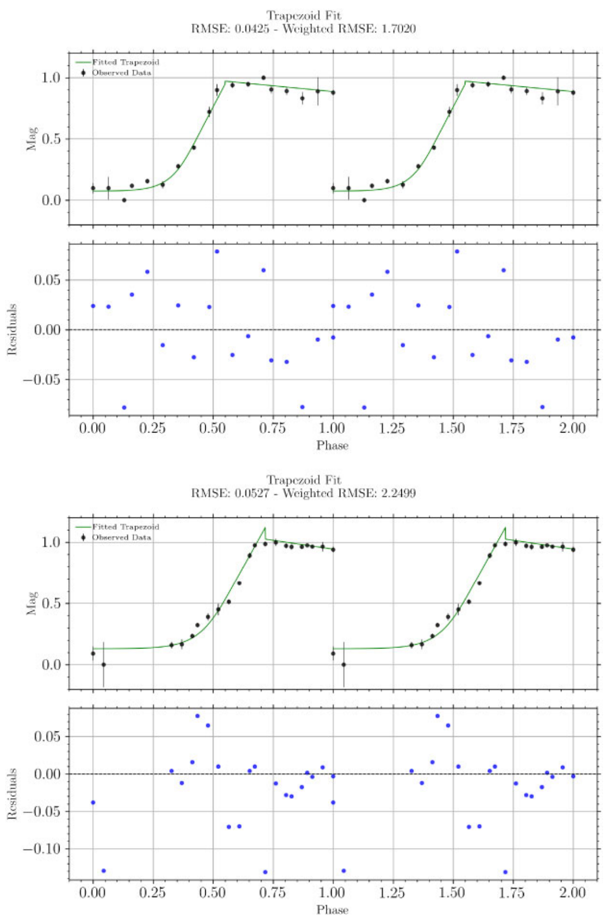

Figure A1. NEOWISE light curves (black points) and the best fit FUor outburst model (green line) for the first two FUor candidates mentioned in the text, Sources 257 (top panel) and 294 (bottom panel). The plots display the light curves twice, from zero to two phase, owing to the code's utility in additionally fitting to periodic signals.

APPENDIX B: ADDITIONAL LIGHT CURVES FROM THE EMBEDDED YSO SAMPLE

Listed in this section are the light curves from the stars not mentioned directly in the text.

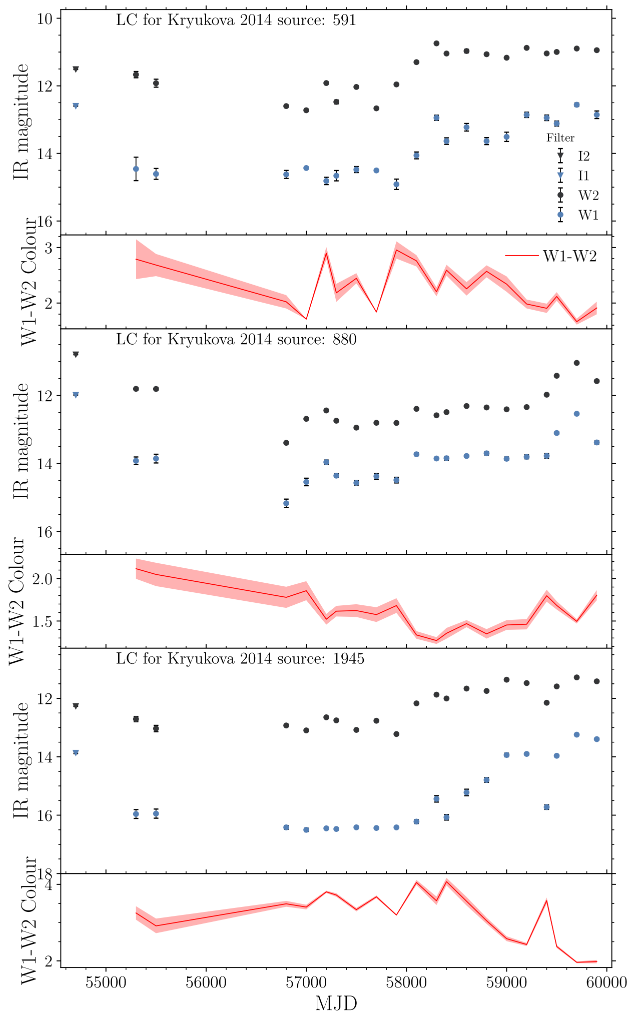

Figure B1. NEOWISE $W1$ and $W2$ light curves for the three long duration sources not detailed within the main text.

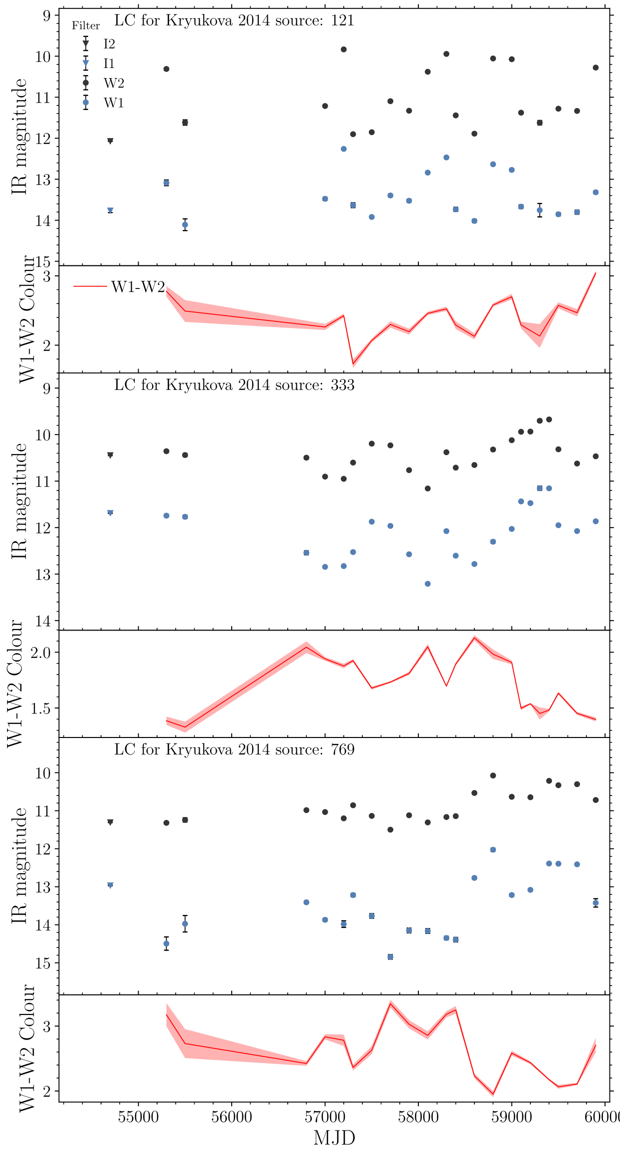

Figure B2. NEOWISE $W1$ and $W2$ light curves for the short-term variables not discussed in the main text.

APPENDIX C: LIGHT CURVES FOR HIGH-AMPLITUDE CLASS I VARIABLE YSOS

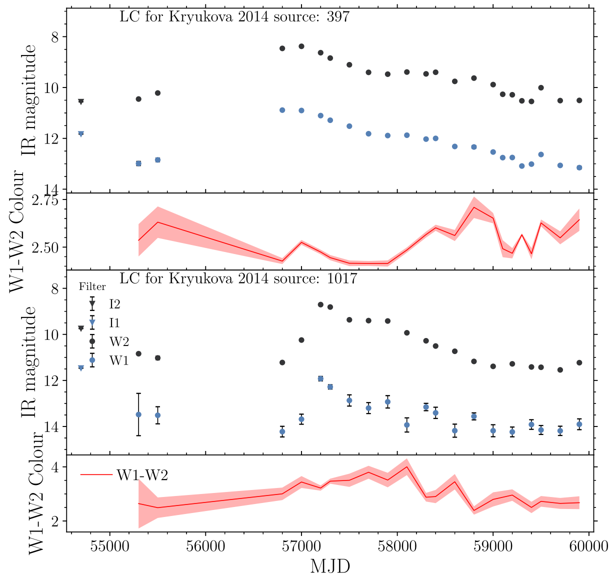

Figure C1. NEOWISE $W1$ and $W2$ light curves for two of the candidate EVs with completed outbursts.

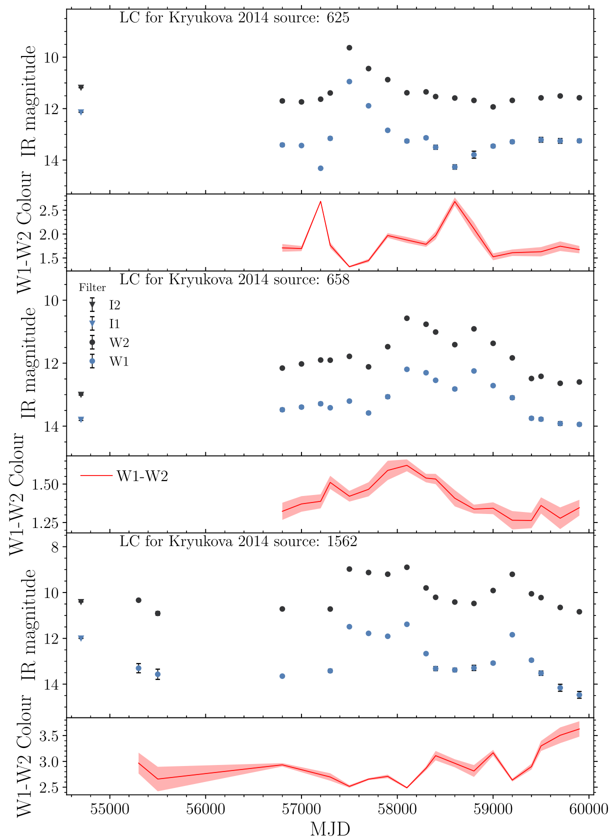

Figure C2. NEOWISE $W1$ and $W2$ light curves for three of the candidate EVs with complex light curves.

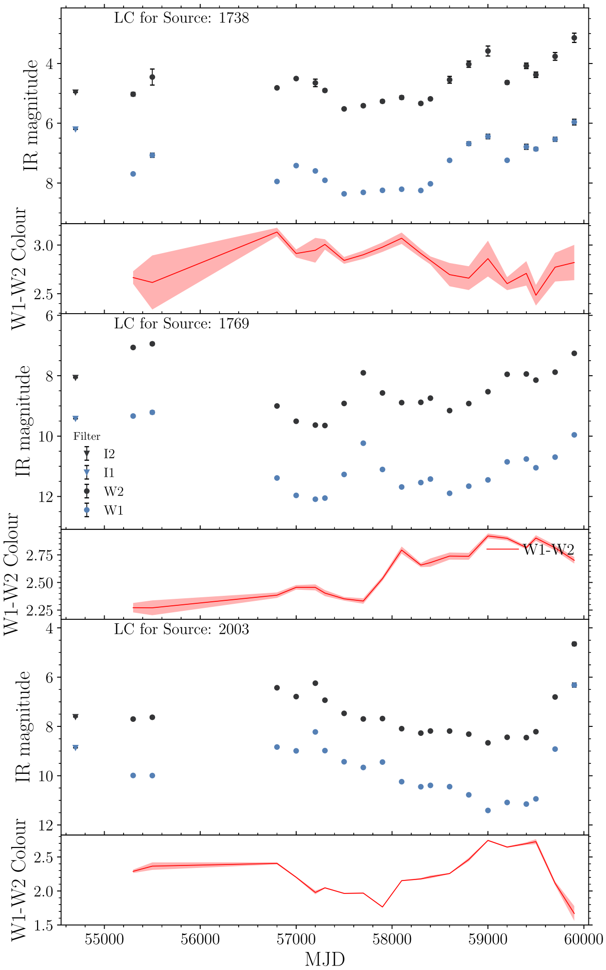

Figure C3. NEOWISE $W1$ and $W2$ light curves for the three stars with uncertain outburst durations.

APPENDIX D: LIGHT CURVES FOR HIGH-AMPLITUDE VARIABLE YSOS FROM SPICY

Listed here are a selection of the NEOWISE MIR light curves for the EXor candidates discussed in Section 3.2. Light curves for all of the stars can be found in the online supplementary material.

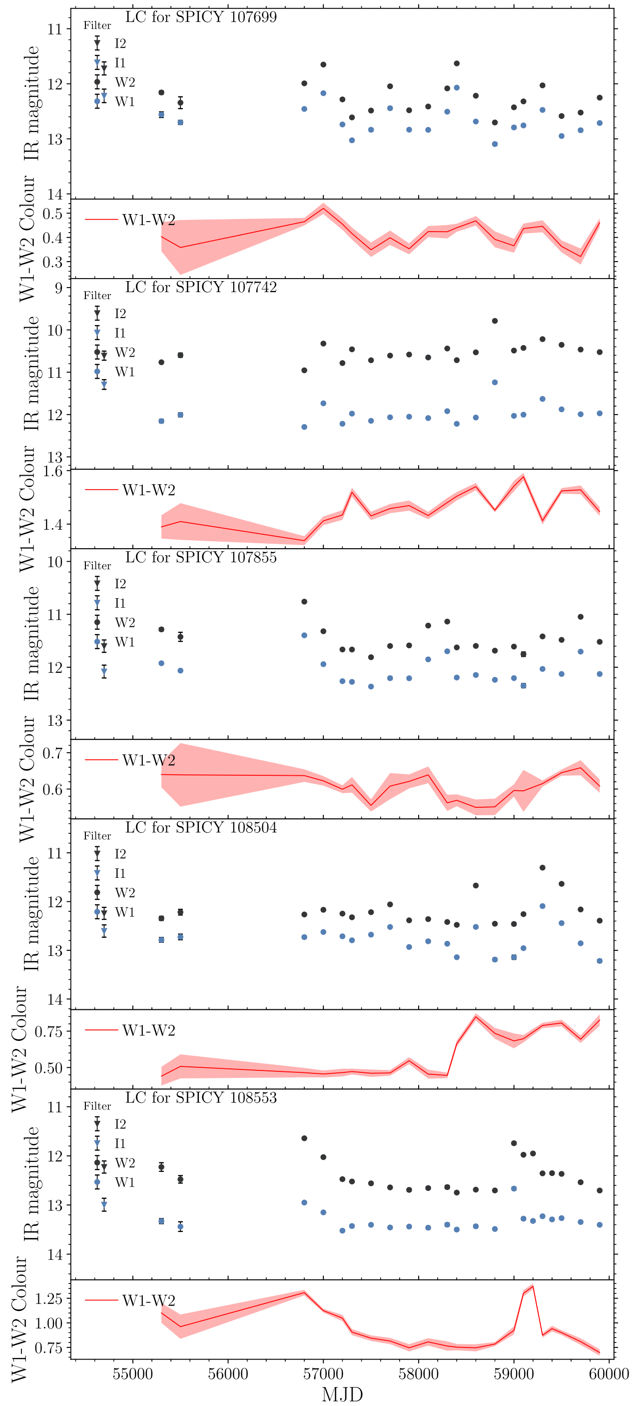

Figure D1. NEOWISE $W1$ and $W2$ light curves for the EXor candidates in the SPICY-selected sample.

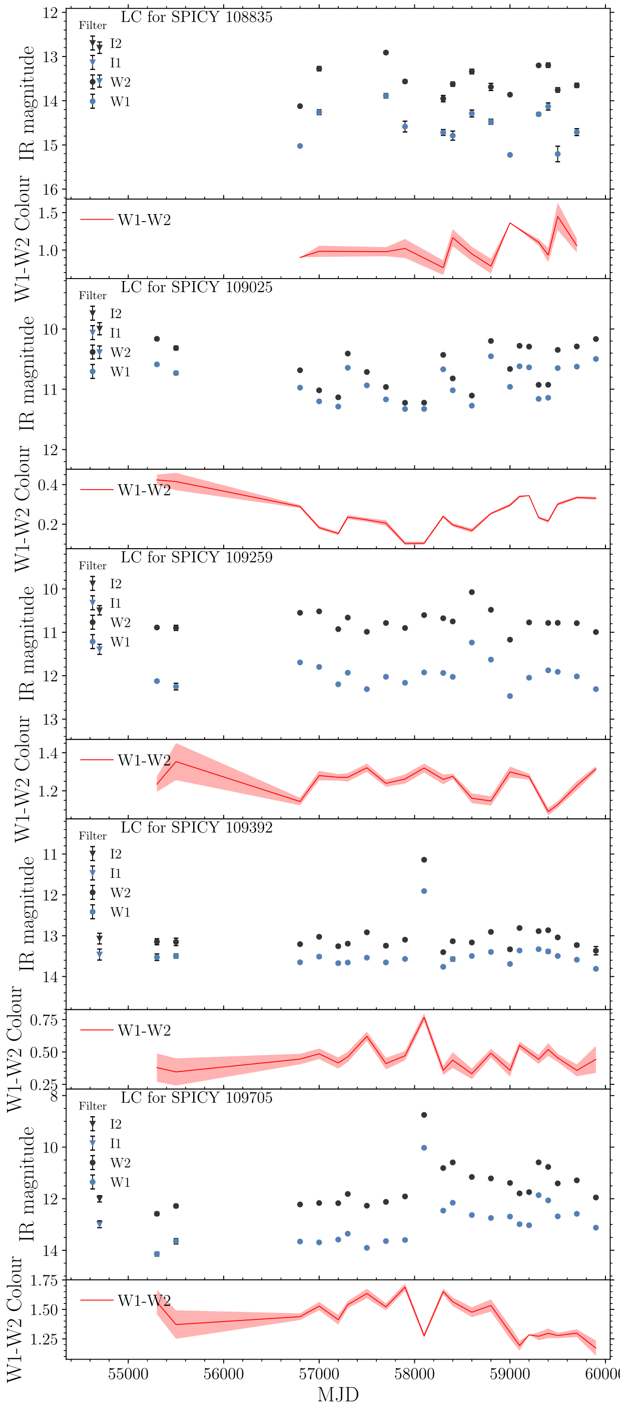

Figure D2. NEOWISE$W1$ and $W2$ light curves for the EXor candidates in the SPICY-selected sample.

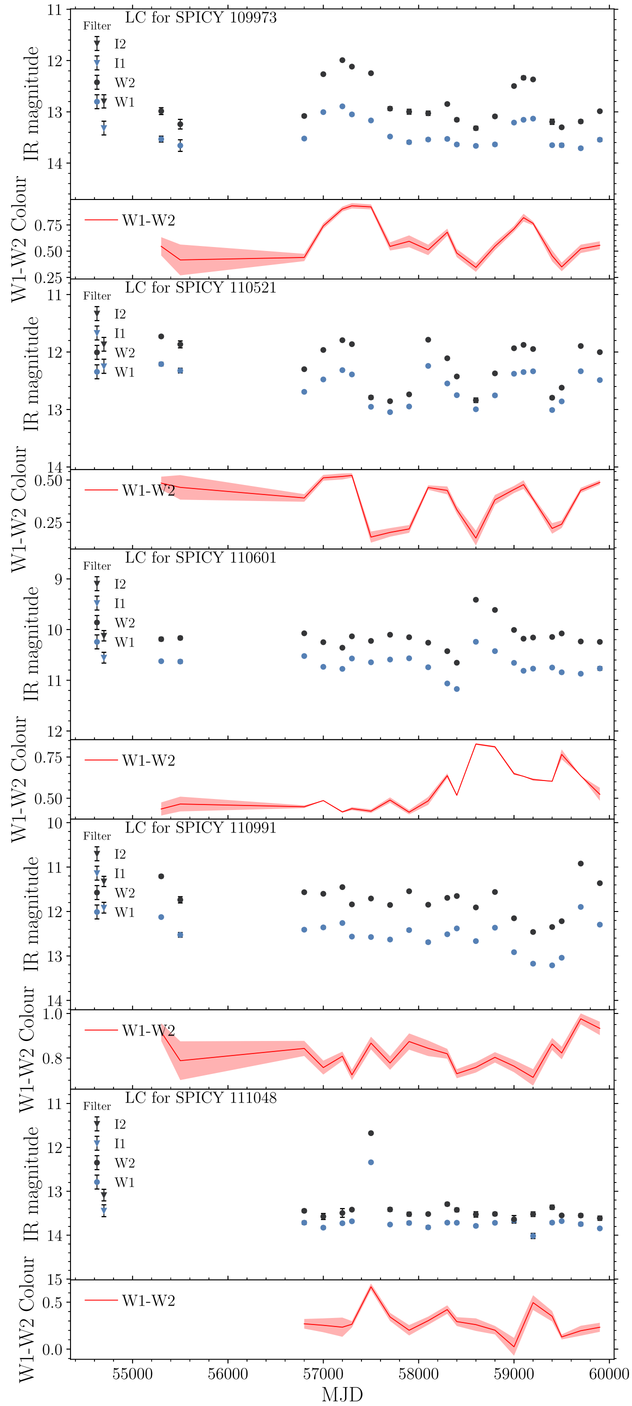

Figure D3. NEOWISE $W1$ and $W2$ light curves for the EXor candidates in the SPICY-selected sample.

This paper has been typeset from a TEX/LATEX file prepared by the author.